UNIVERSITÀ DEGLI STUDI DI MILANO

Facoltà di Medicina e Chirurgia
Dipartimento di Scienze e Tecnologie Biomediche
Settore scientifico disciplinare BIO/10

SCUOLA DI DOTTORATO DI RICERCA IN MEDICINA MOLECOLARE

Curriculum di Oncologia Molecolare

Ciclo XXIII

TESI DI DOTTORATO

Antiproliferative Activity of Cytokinine Derivatives Against HCT-15 Colon and MCF-7 Breast Cancer Cells: Cell Cycle Analysis and BSA &DNA-Binding Study

Il dottorando
Dr. Mehdi Rajabi
Matr. R07902

Il Tutore
Prof. Riccardo Ghidoni

Il Direttore
Prof.ssa Maria Luisa Villa

ANNO ACCADEMICO 2009/2010

ABSTRACT

Background. *N^6-Isopentenyladenosine (iPA) is a member of the cytokinins, a family of plant hormones that regulate plant cell growth and differentiation. iPA is present in mammalian cells in a free form, as a mononucleotide in the cytoplasm, or in a tRNA-bound form. Kinetin Riboside (KR) is devoid of cyclin-dependent kinase inhibitory activity and displayed potent antiproliferative activity against various human cancer cell lines and induced apoptosis in human myeloid leukemia cells. Earlier research has demonstrated that KR antiproliferative and apoptogenic activities are antagonized by pharmacological inhibitors of adenosine kinase (ADK), suggesting that KR bioactivation through metabolic conversion into the nucleotide form is essential for KR cytotoxicity.*

Aims. *Apoptotic mechanism of iPA and KR led us to study in details the dose-dependent cell cycle arrest and apoptogenic effect of iPA and KR on MCF-7 breast and HCT-15 colon cell lines. On the other hand, cell cycle progression or apoptosis can be affected by activation of cell cycle checkpoints in response to DNA damage. We have also studied the interaction of iPA with DNA& BSA as a complementary information related to iPA antiproliferative activity.*

Methods. *Human breast cancer MCF-7 and HCT-15 colon cencer cells were supplied from ATCC. Growth activity of iPA and KR in vitro was evaluated by the Sulforhodamine B (SRB) assay. Apoptosis and cell cycle profile were assessed by flow cytometry. To explore the structural changes of macromoleules on addition of ligands, UV–vis absorbance spectra of macromoleules were measured at different concentrations of ligands.*

Results. *We have calculated an IC_{50} of 12.2 µmol/L for iPA and IC_{50} of 15 µmol/L for KR against MCF-7 and same IC_{50} of 2.5 µmol/L for both iPA and KR against HCT-15. The cell morphology of treated cells was affected by iPA and KR treatment and loss of adhesion, rounding, cell shrinkage and detachment from the substratum. The MCF-7 cell cycle analysis by flow cytometry showed that there was a prominent increase in the amount of sub-G_1/G_0 phase by iPA treatment. At the concentration of 5 µM, KR led to decrease in the percentage of cells in G_0/ G_1 phase, which and increase percentage of cells in S and G_2/M phase. Our result from structural analysis showed interaction of iPA with DNA and the binding constant value $K_{iPA-DNA}=4.4 \times 10^3\ M^{-1}$ together with the shift of UV-vis absorbance suggest that iPA interacts at DNA surface. The BSA binding studies showed that iPA is located along the polypeptide chains with overall affinity constant of $K_{iPA-BSA}=4.9 \times 10^4\ M^{-1}$ and these spectral changes were caused by compound–BSA complex formation, in which compound iPA was strongly bound at the hydrophobic positions of the BSA supported by the hydrophobic interaction.*

Conclusion. *We concluded that the iPA and KR have cytotoxic effect on human MCF-7 and HCT-15 cells with loss of adhesion, rounding, cell shrinkage and detachment from the substratum in treated cells. Cell cycle analysis showed an indication of the inhibition of cell growth through a mechanism of apoptosis. Our result from structural analysis showed interaction of iPA with DNA suggest that iPA interacts at DNA surface and research is required in order to demonstrate that this surface-binding effect may be related to DNA damage in MCF-7 cells.*

INDEX

SIMBOLS LIST

AMP	Adenosine monophosphate
APIPT	Adenosine phosphate-isopentenyltransferase
BA	N^6-benzyladenine
BAR	N^6-benzyladenosine
BSA	Bovine Serum Albumin
CK	Cytokinin
CKs	Cytokinins
CKr	Cytokinin ribosides
cZ	*cis*-Zeatin
DMAPP	Dimethylallyl diphosphate
DMEM	Dulbecco's Modified Eagle Medium
DMSO	Dimethylsulfoxide
FACS	Fluorescence-activated cell sorting
FBS	Fetal Bovin Serum
FCM	Flow cytometry
FPPS	Farnesyl diphosphate synthesis
HBA	HydroxyBenzylAdenine
HBAR	N^6-HydroxybenzylAdenosine
HepG2	Hepto Cellular Carcinoma Cell Line
HMBDP	Hydroxymethylbutenyl diphosphate
HSA	Human Serum Albumin
iPA	N^6-(Δ^2-isopentenyl)adenosine
iPAMP	Isopentenyladenosine-5'-monophosphate
IPT	Isopentenyl transferase
IPCKs	Isoprenoid cytokinins
Kinetin	N^6-furfuryladenine
KR	Kinetin Riboside
MEP	Methylerythritol phosphate
N^6-iA	N^6-(Δ^2-isopentenyl) adenine
PBS	Phosphate buffer saline
PI	Propidium Iodide
TBE	Tris-boratel/EDTA
tZ	*trans*-zeatin
TPA	Tetradecanoylphorbol-13-acetate
tRNA-IPT	tRNA-isopentenyltransferase
VHL	Von Hippel-Lindau

1. INTRODUCTION

1.1. Cytokinins (CKs): Biological role and function

CKs were discovered during the 1950s as substances able to induce the division of plant cells. They are a class of plant hormones that play various roles in many aspects of plant and development, including apical dominance, the formation and activity of shoot stems, leaf senescence, nutrient mobilization, seed germination, root growth, and stress responses. Generally natural CKs (Figure 1.1) are N^6-substituted adenine derivatives and generally the substitution at position N6 consists of an isoprenoid or an aromatic group [1].

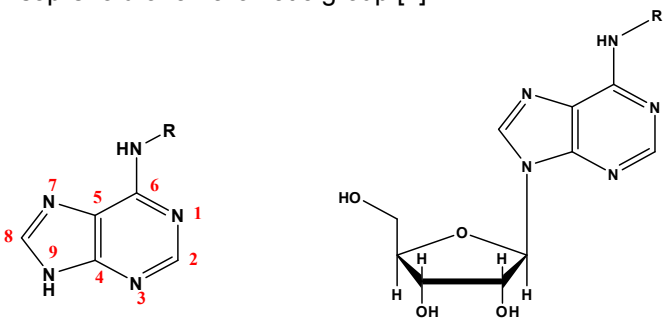

Figure 1.1. *Structure of naturally occurring cytokinin and cytokinin riboside*

kinetin (Figure 1.2) was the first and the best-known of CKs discovered as a degradation product of DNA and was shown to be able to promote cell division in plants [2]. The native kinetin was identified in plant root nodules of *Casuarina equisetifolia* [19] and isolated for the first time in 1950 [1] from autoclaved herring sperm DNA.

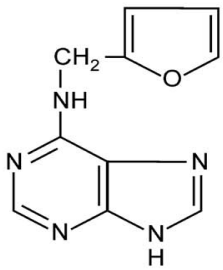

Figure 1.2. *Chemical structure of Kinetin*

Since then, a large number of biochemical, physiological and genetic studies have focused on elucidating the diverse roles of CKs in plant growth and development [3]. Both isoprenoid and aromatic CKs are naturally occurring, with the former more

frequently found in plants and in greater abundance than the latter. Common natural isoprenoid CKs are N^6-(Δ^2-isopentenyl) adenine (N^6-iA), *trans*-Zeatin (*tZ*) and the related stereoisomer *cis*-Zeatin (*cZ*) (Figure 1.3). Among them, the major derivatives generally are *tZ* and N^6-iA as well as their sugar conjugates, but there is a great variation depending on plant species, tissue, and developmental stage [4].

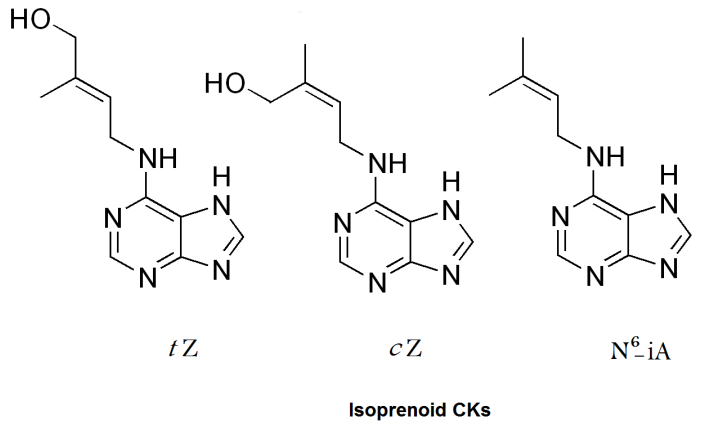

Figure 1.3. *Chemical structure of tZ, cZ, and N^6-iA*

Aromatic CKs, N^6-benzyladenine (BA) and the three isomeric Hydroxybenzyladenine (HBA, topolins) (Figure 1.4) were identified in several plant species including poplar and *Arabidopsis* [5-7] but it is not yet clear whether they are ubiquitous in plants.

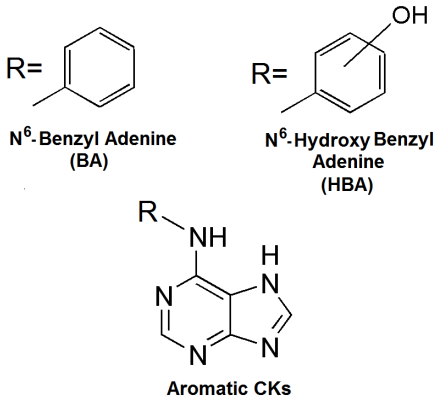

Figure 1.4. *Chemical structure of Aromatic CKs, BA and the three isomeric HBA.*

Usually, for all natural CK nucleobases the corresponding nucleosides, nucleotides, and glycosides (Figure 1.5) have been isolated [4]. Glycosylation of CK has been observed at the N3, N7, and N9 position of the purine moiety as *N*-

glycosides, and at the hydroxyl group of the side chains of *tZ*, *cZ*, and dihydrozeatin as *O*-glucosides or *O*-xylosides (Figure 1.5). *O*-glycosylation is reversible and the deglycosylation is catalyzed by a β-glucosidase. On the contrary, *N*-glycoconjugates are not efficiently cleaved by β-glucosidase [8] and *N*-glycosylation results in a practically irreversible process. The physiological consequences of the differences in stability of *N*-glycosides and *O*-glycosides are not fully understood to date. However, it has been suggested that the readily cleaved *O*-glycosides represent inactive, stable storage forms of CKs [4].

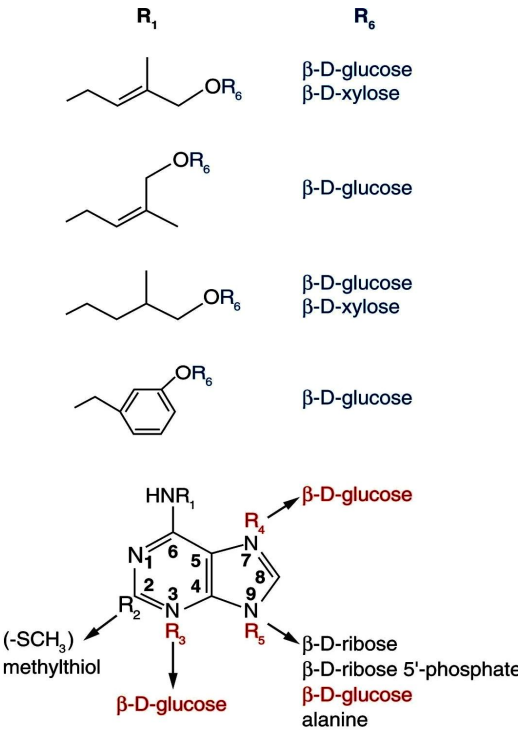

Figure 1.5. *CK conjugates with sugars, sugar phosphates, and others. O-Glycosylation of side chain (colored in blue) is catalyzed by zeatin O-glucosyltransferase or O-xylosyltransferase. N-glucosylation of adenine moiety (colored in red) is catalyzed by cytokinin N-glucosyltransferase.*

1.2. Biosynthesis of CK and CKr

1.2.1. Isoprenoid cytokinins (IPCKs)

CK ribosides and their phosphates predominantly represent the primary products of CK biosynthesis and the concomitant occurrence of CK and the corresponding nucleosides and nucleotides in plant tissues suggests that important metabolic steps are shared with the purine metabolic pathway, i.e., salvage pathway [3] thus,

the metabolic flow from CK nucleotides to the active nucleobases is probably not unidirectional but circular (Figure 1.6).

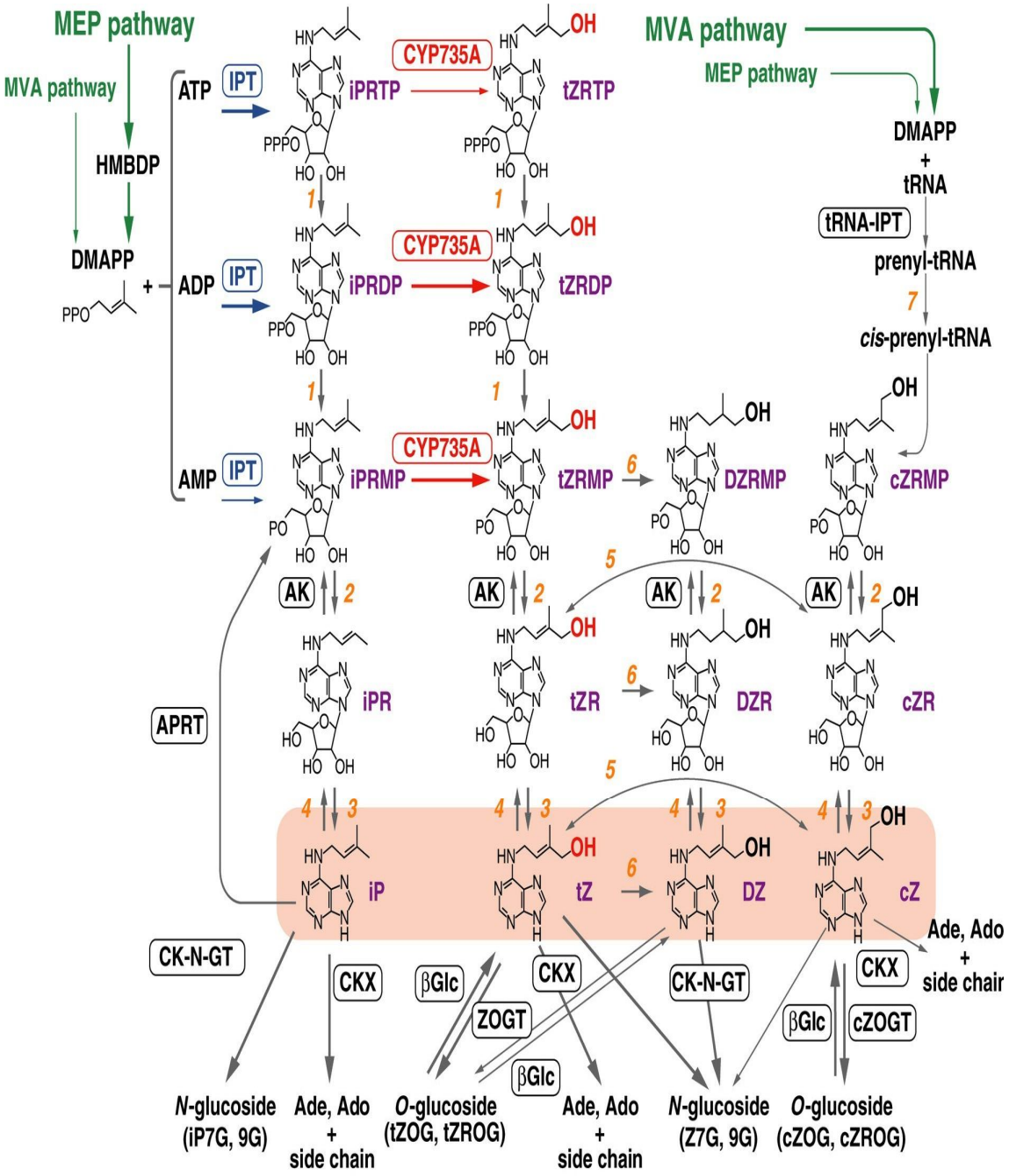

Figure 1.6. *Current model of IPCKs biosynthesis pathways in Arabidopsis. Isoprenoid side chains of N^6-iA and tZ predominantly originate from the MEP pathway, whereas a large fraction of the cZ side chain is derived from the MVA pathway (green arrows).*

The first step in the isoprenoid CK biosynthesis [4] is N-prenylation of adenosine 5'-phosphates (AMP,ADP, or ATP) at the N6-terminus with dimethylallyl diphosphate (DMAPP) or hydroxymethylbutenyl diphosphate (HMBDP); this reaction is catalyzed by adenosine phosphate-isopentenyltransferase (APIPT) (Figure 1.6). CKs may derive from tRNA degradation as well and shortly after the discovery of CKs, it was assumed that tRNA is a major source of CKs because isoprenoid CKs were identified in the hydrolysates of tRNAs [9-11]. Thus, tRNA prenylation could contribute, at least to some extent, to CK production. Early calculations of turnover rates of tRNA led to the conclusion that tRNA degradation was not a major pathway of CKs synthesis [12].

1.2.2. Aromatic cytokinins

BA (Figure 1.7) has been long considered an artificial CK until this compound was isolated from a CK-autotrophic cell culture of anise, *Pimpinella anisum L*.

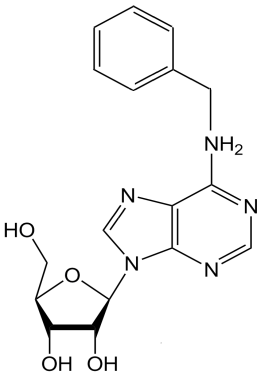

Figure 1.7. *Chemical structure of BAR*

Additional compounds structurally related to BA and BAR, are the three isomeric HBA and HBAR isolated from leaves of *Poplus robusta* and N^6-(o-hydroxybenzyl)-2-methylthio-9-β-D-glucofuranosyladenine isolated from fruits of *Zantedeschia aethiopica robusta* [5]. Despite the fact that BA is one of the most effective and affordable CKs and has been widely used in plant biotechnology for several decades CK research has typically been focused on the isoprenoid class of CKs, typified by zeatin, dihydrozeatin and N^6-iA. The biosynthesis and degradation pathways of aromatic CKs remain to be elucidated, although the mechanisms of glycosylation and of their interaction with the cellular signaling system appear to be

shared with isoprenoid CKs. Apparently, the enzymes and receptors involved recognize members of both groups [13,14]. Indirect evidences on the metabolism of BA [and possibly BAR] seems to indicate that the HBA could be the result of the action of CYP735A or some other P450s on BAR or BA[15].

1.2.3. Kinetin and Kinetin Riboside (KR)

A recent review describes in details the mulptiple biological activities of kinetin [16]. Kinetin has been the first and the best-known CK, isolated for the first time in 1950 [1] from autoclaved herring sperm DNA [2]. For a long time, Kinetin was recognized as a unnatural synthetic product and was found in commercially available DNA, in freshly extracted cellular DNA from human cells, in plant cell extracts and human urine [17,18]. The native kinetin was identified in plant root nodules of *Casuarina equisetifolia* [19]. Recently Kinetin free base and its riboside (KR) (Figure 1.8) has been detected in the endosperm liquid of fresh young coconut fruits [20], at concentrations of 0.31 and 0.33 nM, respectively [21].

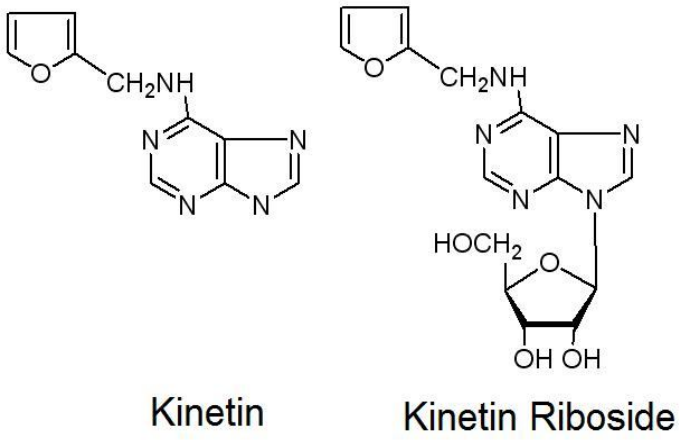

Figure 1.8. *Chemical structure of* K and KR

These findings contribute strongly to answer the question concerning the origin of kinetin and other CKs (Figure 1.9). It has been shown that the cells of legume nodules contain catalytic amounts of iron, which is required for Fenton reaction and formation of hydroxyl radical. The highly reactive oxygen species (ROS) cause degradation of cellular component in nodule extracts. The high yield of Fe-catalyzed Harber-Weiss reaction of deoxyribose damage sustained *in vitro* by the cytosol of bean and cowpea nodules during senescence suggests their potential to generate •OH. These data strongly support the hypothesis that CKs can be recognized as the products of the oxidative metabolism of the cell [22,23]. The proposed mechanism of kinetin formation in DNA *in vivo* starts with the hydroxyl radical oxidation of the deoxyribose residue at the carbon 5' to yield furfural. This

newly formed aldehyde subsequently reacts with the amino group of adenine to form the Schiff base followed by intramolecular rearrangement, which can yield K formation *in vivo* (Figure 1.9) [24].

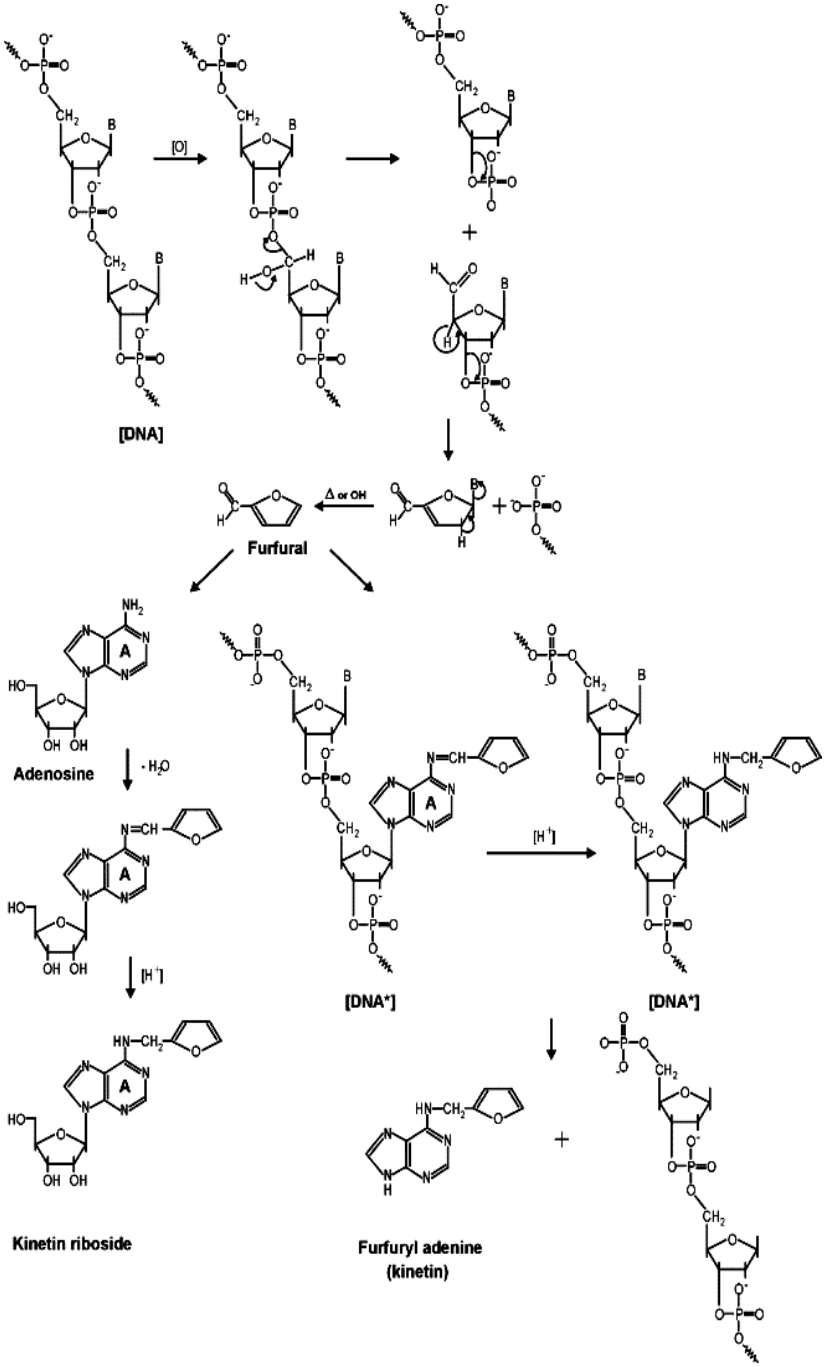

Figure 1.9. *Scheme of synthesis of kinetin and KR. Furfural as a product of DNA oxidation product reacts with ribo or deoxyadenosine.*

1.3. Occurrence of iPA and Kinetin and KR in mammalians

As stated in Section 1.2.3. there are good evidences that Kinetin and KR are formed *in vivo* in mammalians as an important component of a new salvage pathway of hydroxyl radical constituting a 'free radical sink'. By this mechanism, the cell can find a way to respond to oxidative stress, inducing defence mechanisms of maintenance and repair [24]. According to this hypothesis, KR is formed from adenosine to neutralize the harmful properties of hydroxyl radical reaction products, such as furfural that is formed by degradation of sugar residues in DNA and is one of the major routes of cellular damage in addition to the other modifications of nucleic acid bases [25]. In conclusion, although KR is found in mammalians, the product represents an artefact of DNA oxidative stress.

iPA (Figure 1.10) has been found in tRNA from a wide variety of eukaryotic and prokaryotic cells [26].

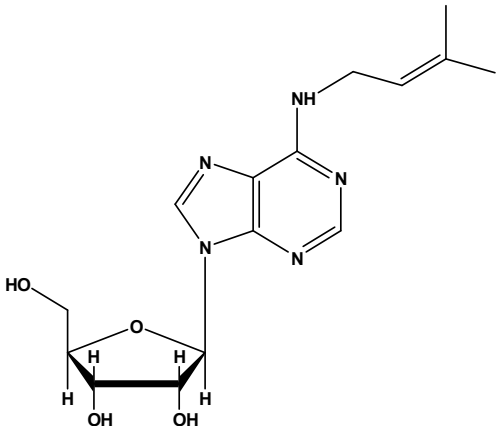

Figure 1.10. *Chemical structure of iPA*

The modified base is derived from 3-methyl-2-buten-1-yl pyrophosphate, an intermediate in cellular isoprenoid biosynthesis. The enzyme that catalyzes the first reaction is Δ^2-isopentenyl pyrophosphate: 5'-AMP Δ^2-isopentenyltransferase commonly referred to as isopentenyl transferase (IPT) and is the enzyme central to all isoprenoid CKs biosynthesis [27]. IPT constitute a family of enzymes that are conserved from micro organisms to mammals and are involved in post transcriptional modification of tRNA, that, in the case of iPA, consists in the addition of the isopentenyl chain to adenosine of the residue 37 of tRNA [28]. iPA is found

adjacent to the 3' end of the anticodon of tRNAs. This modified nucleoside appears only in tRNAs that bind to codons containing uridine as the first base (Figure 1.11).

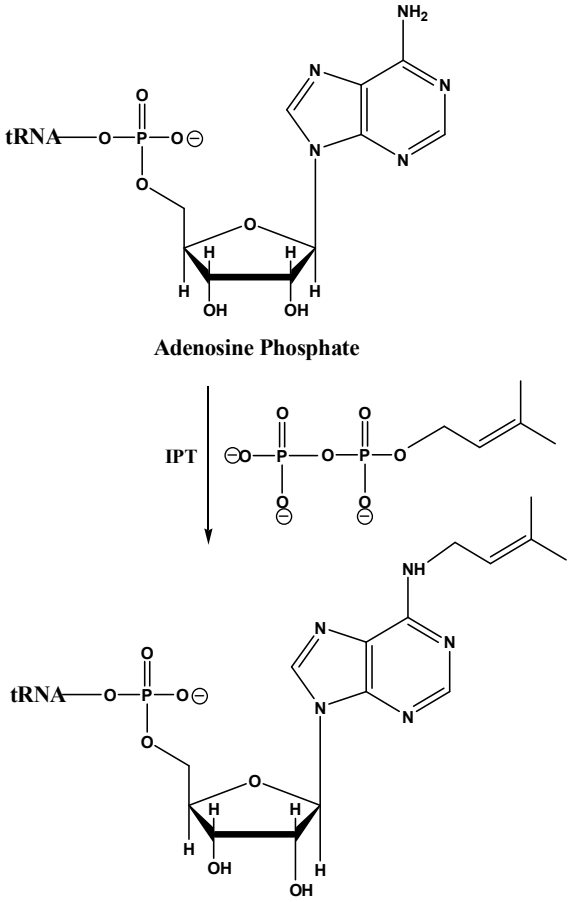

Figure 1.11. *Schematic diagram of the IPT reaction. The acceptor substrate is adenosine residue of tRNA in tRNA–IPT.*

In bacteria, isopentenylated tRNAs have been implicated in the regulation of aromatic acid uptake [29] and aerobiosis [30], whereas the precise role of the modified nucleotide in tRNA metabolism of eukaryotes is unknown. In general, all of RNA modifications are essential in maintaining the correct reading frame of the translational machinery, thus improving fidelity and efficiency of protein synthesis and avoiding errors that could be detrimental for cells [31]. In this respect, it has also been demonstrated that tRNA containing iPA binds more efficiently the ribosome than the unmodified analogues. Therefore the loss of modified nucleotide

from the tRNA can produce pleiotropic effects on accuracy of protein synthesis leading to altered cell proliferation and differentiation [32]. Starting from the consideration that isoprenylated proteins may regulate DNA synthesis and the level of the isoprenylated protein would be low in cells expressing reduced rates of DNA replication It was demonstrated that a 26-kDa protein was present in growing Chinese hamster ovary cells [33] Regenerating liver tissue also exhibited elevated levels of iA26.

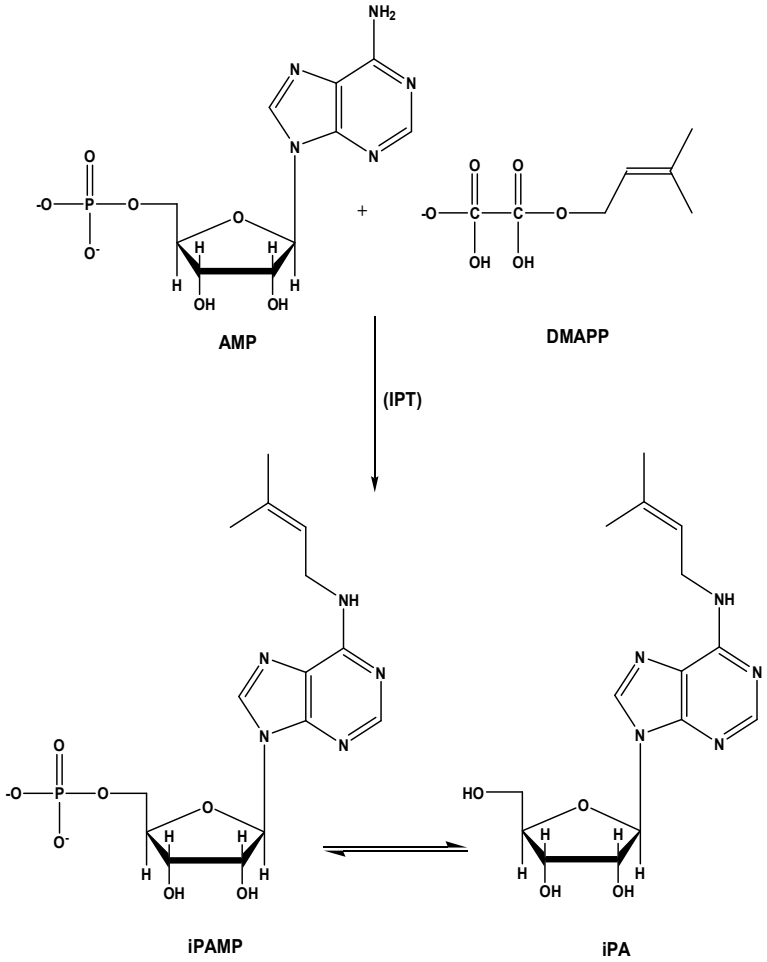

Figure 1.12. *Biosynthesis of iPA in plants. AMP and DMAPP are converted in iPAMP and iPA. IPT is the key regulatory en1zyme of the biosynthesis.*

Thus, the expression of PA26 correlates with cellular proliferation and growth. It was proposed that iPA contains N^6-iP moieties and mediates isoprenoid regulation of DNA synthesis, thus affecting cell proliferation and differentiation in plants and animals. The cellular level of free iPA was not decreased in defective yeast strains possessing mutations that result in severely reduced amounts of isopentenylated

tRNAs. This latter result indicates that free iPA may be derived via a synthetic pathway independent of isopentenylated tRNA degradation. Free, non-tRNA-associated iPA has been observed in yeasts [34] and the cellular level of free iPA was not decreased in defective yeast strains possessing mutations that result in severely reduced amounts of isopentenylated tRNAs. This latter result indicates that free iPA may be derived via a synthetic pathway independent of isopentenylated tRNA degradation. iPA is formed from adenosine monophosphate (AMP) into isopentenyladenosine-5'-monophosphate (iPAMP) and following phosphate hydrolysis (Figure 1.12). The enzyme that catalyzes the first reaction is Δ^2-isopentenyl pyrophosphate: 5'-AMP Δ^2-isopentenyltransferase commonly referred to as IPT and is the enzyme central to all isoprenoid CKs biosynthesis [35].

1.4 Antiproliferation activity of CKr

Crown gall disease, that is characterized by the development of neoplastic growth on the infected plant, affects many dicotyledonous plants and is caused by the soil bacterium *Agrobacterium tumefaciens* [36]. A small region of the Ti plasmid (the *tmr* locus), thought to be involved in phytohormone metabolism in *Agrobacterium tumefaciens*-transformed plant tissue, was cloned and expressed in *Escherichia coli* [37]. By enzyme assay, the *tmr* locus was shown to encode IPT, the enzyme that catalyzes the first step in CK biosynthesis. This established a connection between CKs and induction of callus, a cluster of differentiated plant cells that are immortal and proliferate indefinitely, to re-differentiate into adventitious buds. In this respect, plant callus cells are similar to human cancer cells and CKs were expected to be able to affect the differentiation in some human cancer cells, probably, through a common signal transduction system [38]. Antiproliferative activity has been confirmed by a recent report that examined the control of differentiation and apoptosis of human myeloid leukemia HL-60 cells by CKs and their ribosides CKr [39]. The HL-60 (*Human promyelocytic leukemia cells*) cell line is a leukemic cell line that has been used for laboratory research on how certain kinds of blood cells are formed. The cell line was derived from a 36-year-old woman with acute promyelocytic leukemia at the National Cancer Institute [40]. With this line, spontaneous differentiation to mature granulocytes can be induced by compounds such as dimethyl sulfoxide (DMSO), or retinoic acid. Other compounds like 1,25-dihydroxyvitamin D, 12-O-tetradecanoylphorbol-13-acetate (TPA) and GM-CSF can induce HL-60 to differentiate to monocytic, macrophage-like and eosinophil phenotypes, respectively. The HL-60 cultured cell line provides a continuous source of human cells for studying the molecular events of myeloid differentiation and the effects of physiologic, pharmacologic, and virologic elements on this process. HL-60 cell model was used to study the effect of DNA topoisomerase IIα and IIβ on differentiation and apoptosis of cells [41]. Using HL-60 cell lines, it has been shown that CKs such as kinetin , BA and N^6-iP were very

effective in inducing nitroblue tetrazolium reduction and morphological changes of the cells into mature granulocytes (Table 1.1).

Table 1.1. Effect of adenine analogue on growth of HL-60 cells
Cells were cultures with various concentration of analogues for 5 days. Means of three separate experiments are shown. The IC_{50} is the concentration of compound required for 50% inhibition of cell growth.

Analogues	Growth inhibition (IC_{50} µM)
Purine	**58.4**
1-Methyladenine	**1.713**
3-Methyladenine	**1.172**
2-Aminopurine	**1.341**
Olomoucine	**326.8**
Adenine	**261**
2,6- Diaminopurine	**61.3**
Isopentenyladenine	**47.6**
Kinetin	**48.8**
6-Benzylaminopurine	**67.6**
6-Dimethylaminopurine	**47.2**
trans-Zeatin	**516**
6-n-Hexylaminopurine	**87.5**
6-Anilinopurine	**56.3**
6-Methylaminopurine	**327**
6-Methoxypurine	**744**

On the other hand, examining the coirresponding ribosides CKr, these compounds were more potent than the corresponding CKs for growth inhibition and apoptosis. CKRs greatly reduced the intracellular ATP content and disturbed the mitochondrial membrane potential, consequentially impairing the accumulation of reactive oxygen species. The same effect was not observed for CKs When the cells were incubated with CKRs in the presence of O2. scavenger, antioxidant or caspase inhibitor, apoptosis was significantly reduced and differentiation was greatly enhanced (Table 1.2).

Table 1.2. Effect of adenine analogue on growth of HL-60 cells
Cells were cultures with various concentration of analogues for 5 days. Means of three separate experiments are shown. The IC_{50} is the concentration of compound required for 50% inhibition of cell growth.

Analogues	Growth inhibition (IC_{50} μM)
Adenosine	**685**
Deoxyadenosine	**662**
Isopentenyladenine	**0.972**
Kinetin Riboside	**0.981**
Benzylaminopurine riboside	**0.706**
2,6-Diaminopurine deoxyriboside	**6.23**

Above results suggest that both CKs and CKr can induce granulocytic differentiation of HL-60 cells, but CKr also induce apoptosis prior to the differentiation process. In another study [42], the *in vitro* induction of apoptosis by N6-substituted derivatives of adenine (CKs and analogues) or adenosine (CKr and analogues) in HL-60 cells has been investigated. Using reversed phase HPLC/MS analysis they demonstrated that both N^6-substituted derivatives of adenosine and adenine are phosphorylated within cells to the monophosphate level. While N6-substituted derivatives of adenosine were phosphorylated by adenosine kinase and corresponding mononucleotides were produced in large quantities, N6-substituted derivatives of adenine were converted into the corresponding mononucleotides via the phosphoribosyl transferase pathway, which yielded 50–100 times lower amounts of the mononucleotides than the adenosine kinase pathway. Accordingly, N6-substituted derivatives of adenine were relatively inefficient inductors of apoptosis (Figure 1.13).

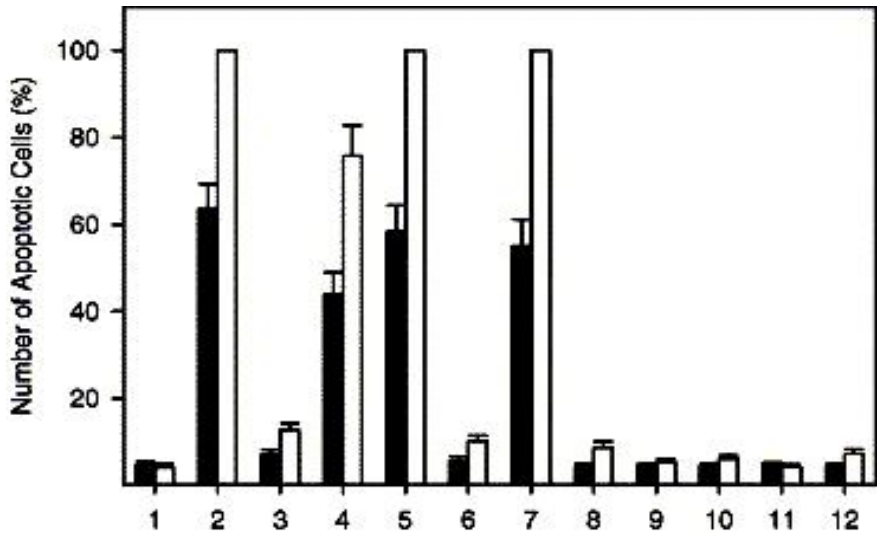

Figure 1.13. *Effect of N^6-substituted derivatives of adenosine or adenine on apoptosis induction in HL-60 cells. Cells were treated with N^6-substituted*

derivatives of adenosine or adenine, as indicated. Cells were incubated for 12 h (black columns) or 24 h (white columns) and the number of apoptotic nuclei was evaluated using fluorescence microscopy. 1-Control (untreated cells), 2-10 μM N^6-benzyladenosine, 3-100 μM N^6-cyclopentyladenosine, 4-10 μM N^6-dimethyladenosine, 5-10 μM KR, 6-100 μM N^6-(4-hydroxy-3-methyl-2-buten-1-yl)adenosine, 7-10 μM iPA, 8-100 μM N^6-benzyladenine, 9-100 μM N^6-dimethyladenine, 10-100 μM kinetin, 11-100 μM N^6-(4-hydroxy-3-methyl-2-buten-1-yl)adenine, and 12-100 μM N^6-iP. The experimental points represent mean values from three replicate experiments with standard deviations.

Inhibitors of adenosine kinase, that abrogated the formation of the monophosphates from N6-substituted derivatives of adenosine, completely prevented cells from going into apoptosis. These results consistently support the idea that pro-apoptotic effects of N6-substituted derivatives of adenosine are related to their intracellular conversion into corresponding mononucleotides which activate apoptosis when accumulated. This accumulation leads to a rapid decrease in ATP production and consequently to apoptosis induction. Nevertheless, the detailed mechanism is unknown. These results proposed an interesting working hypothesis related to a different activity of CKs and their CKr, although this difference were limited only to human myeloid leukemia HL-60 cells. Among examined CKs and related ribosides CKr, it has been shown that BAR, KR and iPA are more effective than related adenine derivatives BA, K or iPA (Table 1 and 2).

1.4.1. iPA Antitumor activiyy *in vitro*.

Nearly forty years ago, Gallo and co-workers [43] observed that iPA can exert a promoting or inhibitory effect on human cell growth, on the bases of used concentration and the cell cycle phase. They reported that iPA is a potent inhibitor or a stimulator of the DNA synthesis, since addition of iPA at μM concentration produced inhibition. Lower concentrations (0.1-1.0 μM) had a stimulatory effect. Moreover they demonstrated that the addition of iPA at increasing times, after cells seeding and proliferation stimulation, determined a decrease of mitotic figures, suggesting that iPA effects depend on the phase of cell cycle. It was also demonstrated that the effects on DNA synthesis are preceded by the inhibition of RNA and protein synthesis. In 1973, Divekar *et al.* demonstrated that iPA is cytotoxic for Sarcoma 180 cells as for the majority of the mammalian cells [44]. It was observed that iPA at the concentration of 22 and 100 μM inhibited the growth of Sarcoma 180 cells (50% and 100% respectively) acting as a potent inhibitor of the uptake of purine and pirimidine nucleosides. Studies performed on the extracts of these cells demonstrated that iPA is a substrate for adenosine kinase and it is also a weak inhibitor of adenosine deaminase, glucose-6-phosphate-dehydrogenase and methylase of mammalian tRNAs. The authors suggested that

iPA cytotoxicity for these cells might be due to its conversion in 5'-monophosphate, that is cytotoxic at high intracellular levels, affecting the enzymes involved in purine metabolism (Figure 1.14). The ability of CKs to induce apoptosis was studied by Meisel *et al.* [45] in several human cell lines and it was observed that iPA was the most active CK, specially with respect to Caco-2 and HL-60 cancer lines. As previously reported, CKr such as KR and iPA inhibited growth and differentiation of human myeloid leukaemia HL-60 cells, inducing their apoptosis [39,42]. Laezza and co-workers [46] demonstrated that iPA in thyroid cell FRTL-5 influences the cAMP dependent organization of the microfilaments. The same authors have later demonstrated that iPA caused a dose-dependent arrest of G0-G1 cell phase transition associated with a reduction of cells in S phase [47] .

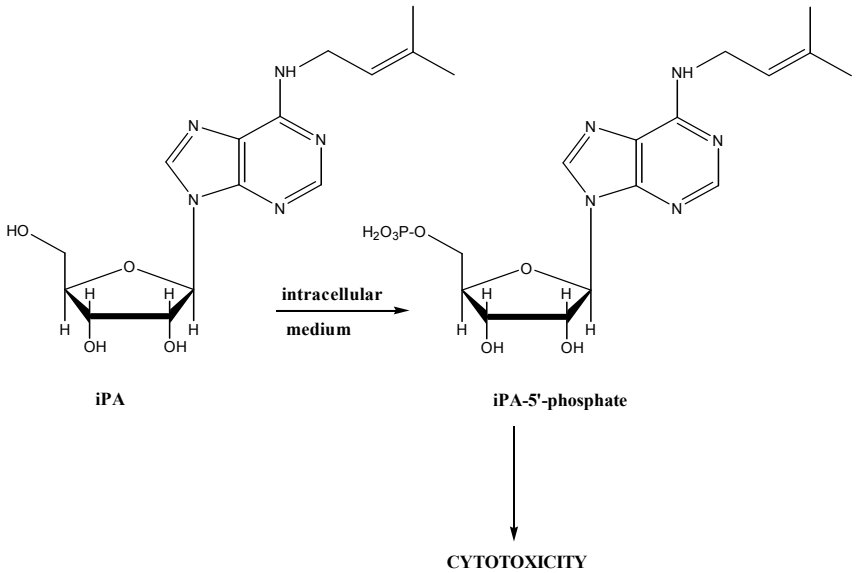

Figure 1.14. *iPA cytotoxicity might be due to its conversion in 5'-monophosphate.*

It was shown that iPA is able to inhibit farnesyl diphosphate synthesis (FPPS) and to affect protein prenylation. This can explain the arrest of tumour cells proliferation in a reversible mode, since the addition of farnesol could reverse the process. This effect was not mediated by the adenosine receptors but was due to a direct modulation of FPPS enzyme activity as a result of its uptake inside the cells.
In 2005 Dragani and coworkers showed by a pharmacogenomic approach that the human tRNA-isopentenyltransferase (TRIT1) gene could be a candidate lung tumor suppressor [48]. tRNA-isopentenyltransferase (tRNA-IPT) catalyses the addition of iPA on residue 37 of tRNA molecules that bind codons starting with uridine [28]. In the cited study [48], TRIT1 expression in normal lung parenchyma was compared with that in A549 lung cancer cells. Cancer cell lines overexpressing the biochemically functional TRIT1 variant were analyzed and, as a result, the TRIT1

gene was identified as a potential negative regulator of lung carcinogenesis. The results obtained by Laezza *et al*. [47] suggesting that the capability of iPA of inhibiting FPPS could concur to arrest tumour cells proliferations was not confirmed by Dragani and co-workers in another study. The antiproliferative activity of iPA in 9 human epithelial cancer cell line derived from different types of malignant tissue was examined [49] and FPPS downregulation in A549 cells was not involved in the antiproliferative activity of iPA. Dragani *et al*. observed complete suppression of clonogenic activity in 8 of the cell lines after exposure to iPA at a concentration of 10 μM. A clonogenic assay is a microbiology technique for studying the effectiveness of specific agents on the survival and proliferation of cells. It is frequently used in cancer research laboratories to determine the effect of drugs or radiation on proliferating tumor cells [50]. Although this technique can provide accurate results, the assay is time-consuming to set up and can only provide data on tumor cells that can grow in culture. The word "clonogenic" refers to the fact that these cells are clones of one another. The experiment involves as major steps plating the cells are in a tissue culture vessel and allowed to grow, production of colonies, and tratment of the formed colonies (the colonies produced are fixed, stained, and counted). Any type of cell could be used in an experiment, but since the goal of these experiments in oncological research is the discovery of more effective cancer treatments, human tumor cells are a typical choice. The cells either come from prepared cell lines, which have been well-studied and whose general characteristics are known, or from a biopsy of a tumor in a patient [51]. The cells are put in petri dishes or in plates which contain several circular "wells" and counting the cell colonies is usually done under a microscope. Figure 1.15 shows A549 colonies in untreated and 10 μM iPA-treated cells for 24, 48 or 72 h and maintained thereafter in culture medium alone until the end of the experiment.

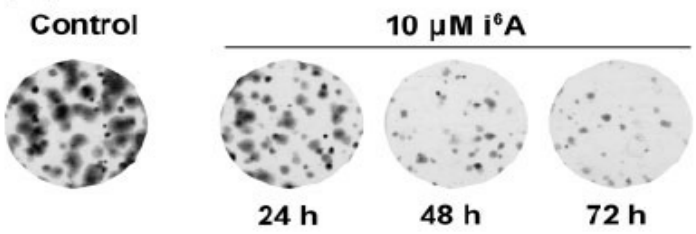

Figure 1.15. *Representative plates showing A549 colonies in untreated and 10 μM iPA-treated cells for 24, 48 or 72 h and maintained thereafter in culture medium alone until the end of the experiment*

In the cited work [49], a complete suppression of clonogenic activity in 8 of the lines after exposure to iPA was observed at a concentration of 10 μM. Specifically, iPA was effective with human lung cancer cell lines NCI-H520 and NCI-H596, with breast cancer cell lines MDA-MB-361 and MCF-7, and nasal septum squamous

cell carcinoma cell line RPMI 2650 (Figure 1.16). Human lung cancer cell lines A549 and Calu-3, hepatocellular carcinoma cell line HepG2, and colorectal adenocarcinoma cell line HT-29 were also examined (Figure 1.17). Only the cell line HT-29 derived from a colorectal cancer showed a significant but incomplete inhibition upon iPA treatment, with about 70% colony inhibition as compared to untreated control cells.

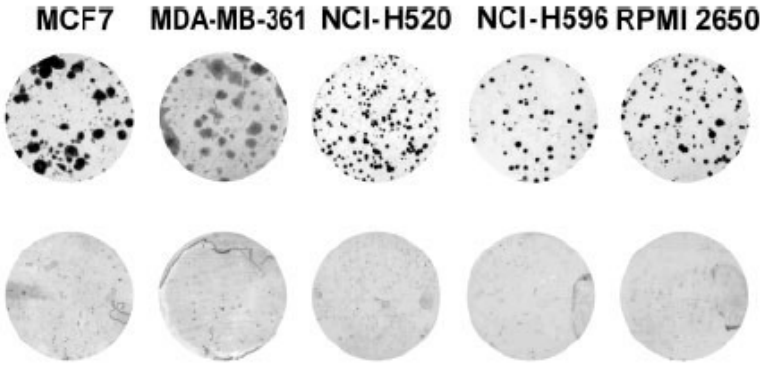

Figure 1.16. *Representative plates showing colony formation in untreated (top) or 10 μM iPA-treated (bottom) cancer cell lines of different tissue origins.*

The incomplete inhibition of HT-29 cell clonogenic activity might rest in reduced intracellular adenosine kinase activity, with a consequent slower or decreased formation of intracellular iPA-5'-monophosphate which appears to be the ultimate cytotoxic agent [44]. Alternatively, a lower permeability of these cells to iPA, as compared to the other cell lines, cannot be excluded.

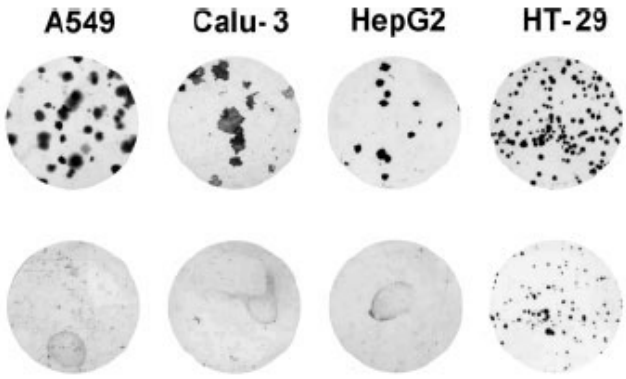

Figure 1.17. *Representative plates showing colony formation in untreated (top) or 10 μM iPA-treated (bottom) cancer cell lines of different tissue origins. Only colorectal adenocarcinoma cell line HT-29 growth was not completely inhibited.*

Differently from the results obtained with the human myeloid leukemia cell line HL-60 [39], only a modest increase in apoptosis after iPA treatment was revealed in epithelial cancer lines [48,49]. Indeed, in lung cancer cells tumor growth suppression appears to be mediated by inhibition of cell proliferation due to a block of DNA synthesis rather than apoptosis. These findings are consistent with the reported iPA-induced inhibition of proliferation of rat thyroid tumour cells [46,47,52]. Moreover, iPA is able to cause a pronounced change in the morphology of A549 cells. This is associated to disorganization of actin fibers in the cytoplasm (Figure 1.18) and overall results suggest a stress situation for that cell line under iPA exposure.

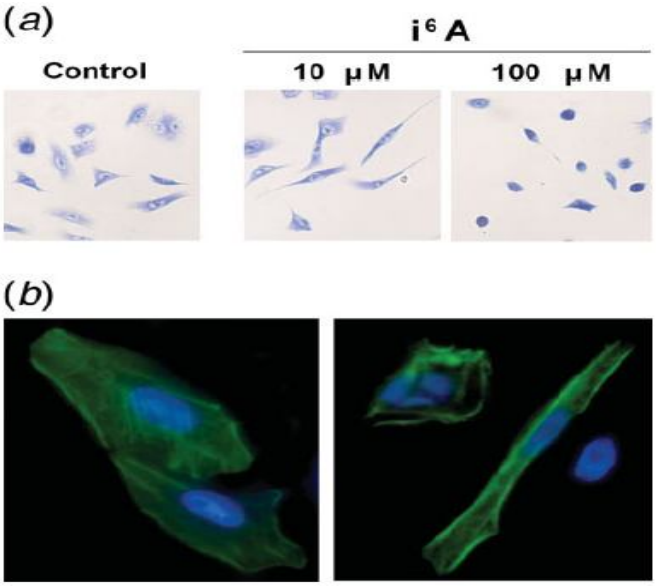

Figure 1.18. *Changes in cell morphology and in distribution of actin fibers by iPA treatment of A549 cells. (a) Representative microscopic fields of A549 cells stained with 10% Giemsa 18 h after treatment with 0, 10 or 100 µM iPA. (b) Untreated (left) and 100 µM iPA-treated (right) cells showing fuorescence-labeled actin fibers (green) and DAPI nuclear staining (cyan).*

In 2009, Laezza e al. studied iPA effects on DLD1 human colon cancer cells [52]. iPA suppressed the proliferation of cells through inhibition of DNA synthesis, causing a cell cycle arrest that correlated with a decrease in the levels of cyclins A, D1 and E with a concomitant increase in the levels of cyclin-dependent kinase inhibitor p21waf and p27kip1. iPA induced apoptosis through an increase in the number of annexin V-positive cells, a downregulation of antiapoptotic products and caspase-3 activation. The apoptotic effects of iPA were accompanied by sustained

phosphorylation and activation of c-jun N-terminal kinase (JNK) that induced phosphorylation of c-jun.

1.4.2. *in vitro* antitumor activity of KR

Ony a few, recent reports are available in literature about in vitro antitumor activity of KR. In the seminal work by Ishii and coll., it has been reported that kinetin riboside together with isopentenyladenosine, and benzylaminopurine riboside were more potent than the corresponding N6-substituted purines for growth inhibition and apoptosis of human myeloid leukemia HL-60 cells [39]. It has also been reported that, at 1.5 and 0.2 μM concentration, kinetin riboside KR shows cytotoxic effects on M4 Beu human and B16 murine melanoma cells. At these concentrations, cell growth is reduced by 50%, respectively, but there was no effect on the growth of mice leukaemia P388. KR is toxic at the dose of 25 mg/kg [53]. More recent results have shown that KR induces apoptosis in HeLa and mouse melanoma B16F-10 cells [54]. B16F10 mouse melanoma cell line is an established model for metastasis [55-57]. HeLa cell is a cell type in an immortal cell line used in scientific research. It is one of the oldest and most commonly used human cell lines [58]. The line was derived from cervical cancer cells taken from a patient named Henrietta Lacks, who eventually died of her cancer on October 4, 1951. The cell line was found to be remarkably durable and prolific as illustrated by its contamination of many other cell lines used in research [59]. HeLa cells are termed “immortal” in that they can divide an unlimited number of times in a laboratory cell culture plate as long as fundamental cell survival conditions are met (i.e. being maintained and sustained in a suitable environment). There are many strains of HeLa cells as they continue to evolve by being grown in cell cultures, but all HeLa cells are descended from the same tumor cells removed from Mrs. Lacks. It has been estimated that the total number of HeLa cells that have been propagated in cell culture far exceeds the total number of cells that were in Henrietta Lacks' body. HeLa cells were used by Jonas Salk to test the first polio vaccine in the 1950's. Since that time HeLa cells have been used for "research into cancer, AIDS, the effects of radiation and toxic substances, gene mapping, and countless other scientific pursuits". According to author Rebecca Skloot, by 2009, "more than 60,000 scientific articles had been published about research done on HeLa, and that number References was increasing steadily at a rate of more than 300 papers each month. The apoptotic effect of KR in HeLa and mouse melanoma B16F-10 cells was explained through disruption of the mitochondrial membrane potential, induction of the release of cytochrome c, and activation of caspase-3. Tumor growth in mice was dramatically suppressed by KR. In contrast, human skin fibroblast CCL-116 and bovine primary fibroblast cells show resistances to KR and no significant changes in Bad, Bcl-XL, and cleaved PARP were observed. Reported data suggest that KR selectively induces apoptosis in cancer cells through the classical mitochondria dependent apoptosis pathway [54]. More recent

results have added information on the mechanism of KR-induced antiproliferation and apoptosis of cancer cell lines. It has very recently demonstrated that KR induced marked suppression of *CCND2* transcription and rapidly suppressed cyclin D1 and D2 protein expression in primary myeloma cells and tumor lines, causing cell-cycle arrest, tumor cell–selective apoptosis, and inhibition of myeloma growth in xenografted mice [60]. In another very recent study, a hypothesis about the cytotoxic effects of KR was tested. KR effects may involveinterference with DNA integrity and cellular energy status leading to stress response gene expression and cell cycle arrest. Results obtained from MiaPaCa-2 pancreas carcinoma, A375 melanoma, and various other human cancer cell lines indicate that massive ATP depletion and induction of genotoxic stress occurs rapidly in response to KR exposure. This is followed by early upregulation of HMOX1, CDKN1A, and other DNA damage/stress response genes. These data suggest that early induction of genotoxicity and energy crisis are causative factors involved in KR cytotoxicity and anticancer activity [61] (Table 1.3).

Table 1.3. FAdo anti-proliferative activity against primary human skin cells and human melanoma, colon, and pancreas cancer cell lines.

IC_{50} values of FAdo-induced inhibition of proliferation of human skin cells [primary keratinocytes (HEK) and dermal fibroblasts (Hs27)] and melanoma (A375, G361, and LOX), colon (HT29 and HCT116), and pancreas (MiaPaCa-2) cancer cell lines were determined in proliferation

Cell line	**IC_{50} (FADo, µM)**
G361	1.52
LOX	0.16
A375	0.28
HT29	3.00
HCT116	0.27
MiaPaCa-2	6.23
HEK	0.11
Hs27	0.18

2. RATIONAL

2.1 Cancer

Cancer is a class of diseases in which a cell, or a group of cells display uncontrolled growth (division beyond the normal limits), invasion (intrusion on and destruction of adjacent tissues), and sometimes metastasis (spread to other locations in the body via lymph or blood). These three malignant properties of cancers differentiate them from benign tumors, which are self-limited, and do not invade or metastasize. Most cancers form a tumor but some, like leukemia, do not. The branch of medicine concerned with the study, diagnosis, treatment, and prevention of cancer is oncology [62]. Nearly all cancers are caused by abnormalities in the genetic material of the transformed cells. These abnormalities may be due to the effects of carcinogens, such as tobacco smoke, radiation, chemicals, or infectious agents. Other cancer-promoting genetic abnormalities may be randomly acquired through errors in DNA replication, or are inherited, and thus present in all cells from birth. The heritability of cancers is usually affected by complex interactions between carcinogens and the host's genome. New aspects of the genetics of cancer pathogenesis, such as DNA methylation, and microRNAs are increasingly recognized as important. Genetic abnormalities found in cancer typically affect two general classes of genes. Cancer-promoting "oncogenes" are typically activated in cancer cells, giving those cells new properties, such as hyperactive growth and division, protection against programmed cell death, loss of respect for normal tissue boundaries, and the ability to become established in diverse tissue environments. "Tumor suppressor genes" are then inactivated in cancer cells, resulting in the loss of normal functions in those cells, such as accurate DNA replication, control over the cell cycle, orientation and adhesion within tissues, and interaction with protective cells of the immune system (Figure 2.1) [63-64].

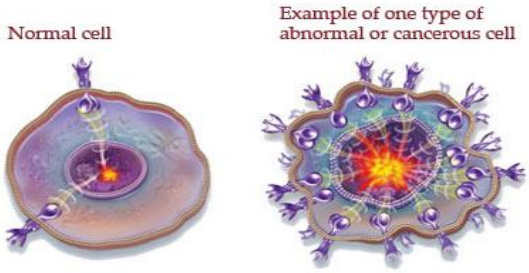

Figure 2.1. *A cancerous cell looks and acts differently from a normal cell (and may have molecules on its surface that are different in number or type from those on a normal cell).*

2.2 Chemotherapy

Chemotherapy is a general term for treatments that use chemical agents (drugs) to kill cancer cells. Many different kinds of drugs are used, either alone or in combination, to treat different cancers. The specific drug or combination used is chosen to best combat the type and extent of cancer present. Chemotherapy drugs are given for several reasons: i)To treat cancers that respond well to chemotherapy, ii) To decrease the size of tumors for easier and safer removal by surgery, iii)To enhance the cancer-killing effectiveness of other treatments, such as radiation therapy, iv)In higher dosages, to overcome the resistance of cancer cells, v)To control the cancer and enhance the patient's quality of life. Healthy normal cells in the body grow and divide in an orderly manner to replace old or damaged cells. Cancer cells have lost that capacity and divide out of control. Chemotherapy drugs work by interfering with the ability of cancer cells to divide and reproduce themselves. Chemotherapy can be delivered by the bloodstream to reach cancer cells all over the body, or it can be administered directly to specific cancer sites. Each chemotherapy drug works in a different way to prevent cells from growing. Often a combination of drugs will be used, with each drug attacking the cancer cells in a different way. This decreases the possibility that cancer cells will survive, become resistant and continue to grow [65-66].

2.3 MCF-7 breast cancer

In 1970, the MCF-7 cell line was derived from a pleural effusion of a patient with metastatic breast cancer [67] and was later recognized as the first hormone-responsive breast cancer cell line [68]. The usefulness of the MCF-7 cell line as an investigative tool led to its adoption in laboratories worldwide and several decades of use in independent laboratories have facilitated the evolution of distinct MCF-7 lineages [69]. Documented differences include the ability to undergo DNA fragmentation, differential sensitivities to estrogens and anti-estrogens, differential expression of estrogen receptors (ER), ER-mRNA, progesterone receptors and differences in tumorigenicity and proliferative rates. It has been well established that the MCF-7 cell line is a novel tool for the study of breast cancer resistance to chemotherapy, because it appears to mirror the heterogeneity of tumor cells *in vivo* [70]. In this respect, it has already been proved that breast cancer cell lines are considered as representative models of transformed cells *in vivo* [71]. In addition to retaining their estrogen sensitivity, MCF-7 cells are also sensitive to cytokeratin. They are unreceptive to desmin, endothelin, GAP, and vimentin. When grown in vitro, the cell line is capable of forming domes and the epithelial like cells grow in monolayers. Growth can be inhibited using tumor necrosis factor alpha (TNF alpha), and treatment of MCF-7 cancer cells with anti-estrogens can modulate insulin-like growth factor finding protein's, which ultimately have the effect of a reduction in cell growth.

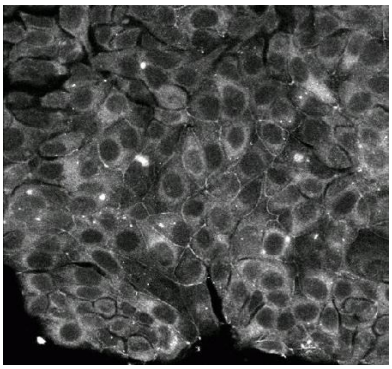

Figure 2.2. *Cell shape of MCF-7 breast cancer cell line*

2.4 HCT-15 a colorectal cancer cell line

Colorectal cancer is the second leading cause of cancer death in the United States[72]. Despite advances in medical practices and chemotherapeutic protocols, survival rates in cases of colorectal cancer have changed little over the last 20 years. HCT-15 cells have mutant p53. Mutated p53 is often expressed in variety of human tumors and contribute to malignant process by loss of tumor suppressor function and gain of novel functions that enhance transformed properties of cells [73]. Swamy *et al* [74] reported that celecoxib increases nuclear localization of active p53. The treatment of celecoxib in HCT-15 cells might involve inhibition of function of mutated p53.

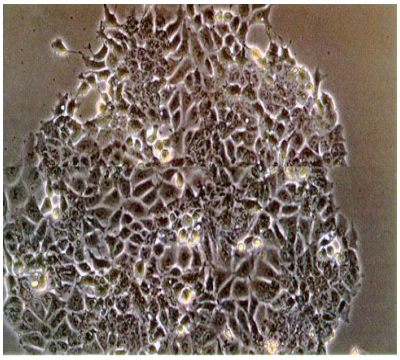

Figure 2.3. *Cell shape of HCT-15 colon cancer cell line*

2.5 Binding study of macromolecules

Macromolecules in the body form noncovalent associations, such as DNA-protein or protein-protein complexes, that control and regulate numerous cellular functions. Understanding how changes in the concentration and

conformation of these macromolecules can trigger physiological responses is essential for researchers developing drug therapies to treat diseases affected by these imbalances.

2.5.1 Drug-DNA interaction

DNA as carrier of genetic information is a major target for drug interaction [75] because of the ability to interfere with transcription (gene expression and protein synthesis) and DNA replication [76], a major step in cell growth and division [77]. The latter is central for tumorigenesis and pathogenesis [78]. Thanks to the work of James Watson, Francis Crick, Linus Pauling, and many other scientists, we now know that DNA is a double helix (spiral) molecule, consisting of two complementary strands of sugar-phosphate groups with bases attached (*Figure 2.4)*.

Figure 2.4. *Francis Crick was a pre-doctoral student of James Watson. They did their research in 1951 at Cambridge University in England.*

The sequence of bases (A, G, C, and T) provide all the genetic information needed to carry out the cell's activities. A mutation is a permanent change in the DNA. A mutation can arise spontaneously without apparent cause, or in response to radiation, ultraviolet light, certain chemicals, or viruses. Some mutations involve the substitution of one base pair for another, for example inserting a G-C where there should be a T-A pair. In other cases, one or more base pairs can be added to, or removed from, the chain. Sometimes huge segments are altered, rearranged, or misaligned. Mutations can lead to cell death, to alterations in the way a cell functions, or in some cases to cancer. This may be because treatment is difficult, there may be no cure, and the disease seems to strike without warning.

There are three principally different ways of drug-binding. First, through control of transcription factors [79,80] and polymerases [81, 82, 83]. Here, the drugs interact with the proteins that bind to DNA. Second, through RNA binding to DNA double helices to form nucleic acid triple helical structures or RNA hybridization (sequence specific binding) to exposed DNA single strand regions forming DNA-RNA hybrids that may interfere with transcriptional activity. Third, small aromatic ligand molecules that bind to DNA double helical structures by (i) intercalating between stacked base pairs thereby distorting the DNA backbone conformation and interfering with DNA-protein interaction or (ii) the minor groove binders. The latter cause little distortion of the DNA backbone (Figure 2.5). Both work through non covalent interaction. The small ligand drug approach offers a simple solution. The synthesis and screening of synthetic compounds that do not exist in nature, work much like pharmacological ligand for cell surface receptors in excitable tissue, and appear to be more readily delivered to cellular targets than large RNA or protein ligands. The lack of sequence specificity for intercalating molecules, however, does not allow to target specific genes, but rather certain cellular states or physiological and pathological conditions, like rapid cell growth and division that can be selectively suppressed as compared to non growing or slowly growing healthy tissue [84-92].

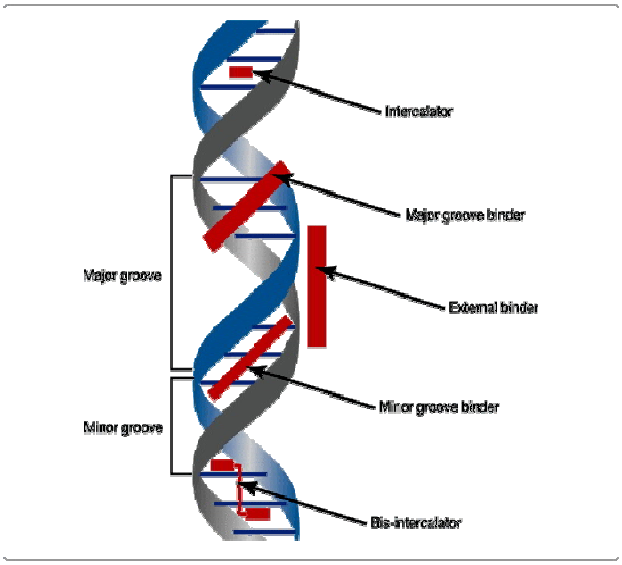

Figure 2.5. Schematic diagram showing the different binding modes of ligands to DNA.

2.5.2 Conformation investigation of Bovine Serum Albumin

Serum albumins are the major soluble protein constituents of the circulatory system and have many physiological functions[93-96]. Binding to albumin is an important

factor in the solubilization and transportation of drugs in blood [97-99] and the molecules that have higher affinity for serum albumin and show preferential binding sites on serum albumin may find important therapeutical applications[100]. The most important property of this group of proteins is that they serve as transporters for a variety of compounds. BSA (Figure 5.18) has been one of the most extensively studied of this group of proteins, particularly because of its structural homology with human serum albumin (HSA) [101-103]. Over the past years, studies on the interactions between drugs and BSA in aqueous solution have attracted intense attentions [104-109].

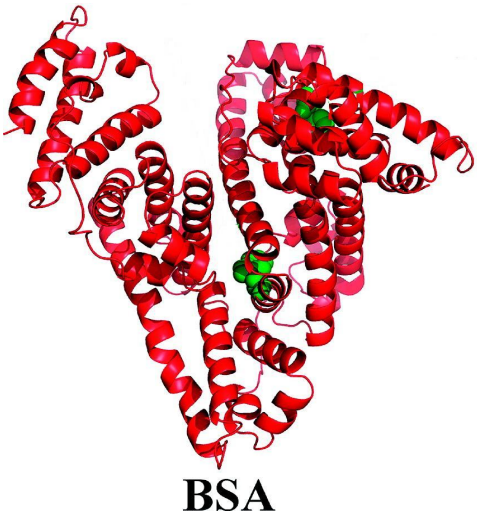

Figure 2.5. *Structure of BSA*

2.6 Rational of this work

Studing on cytotoxic effect of antiproliferative agents on human cancer cell lines that cause apoptotic morphological changes in cells is very interesting in molecular biological chemistry field. The cell cycle analysis by flow cytometry with increase of hypoploid DNA is an indication of the inhibition of cell growth through a mechanism of apoptosis that has been suggested also for other cell lines [39, 46-47]. On the other hand, the connection between DNA damage and apoptosis is supported by a large body of literature [110,111] and also plasma protein binding is one major determinant of the distribution of chemicals in the body. *In vitro*, in cell cultures for example, media often are supplemented with up to 20% (v/v) serum and in those cases the distribution of chemicals can also be determined by protein binding. Binding to serum components in the medium can reduce the availability of chemicals in cell culture systems, which means that the freely dissolved concentrations are lower than the nominal ones. In most cases *in vitro* potency data, used to characterise the biological activity of chemicals, are based on nominal concentrations and not on the actual effective freely dissolved

concentrations. As consequence binding to serum components in the medium also affects potency data obtained with cell cultures. The dependency of in vitro potency data upon serum or albumin content of the medium has been shown frequently [112-114]. At present work, As a complementary information related to the antiproliferative activity, no clear evidence of cytokinines-induced DNA damage and protein structural analysis has been demonstrated.

3. AIMS

CKs are purine derivatives with potential anticancer activity originally discovered as phytohormones that promote cell division, leaf expansion, and callus cell redifferentiation, early and recent experimental evidence suggests that naturally occurring and synthetic CKs target human cancer cells through anti-proliferative, apoptogenic, and differentiation-inducing activities.

iPA is a member of the CKs, a family of plant hormones that regulate plant cell growth and differentiation. iPA is present in mammalian cells in a free form, as a mononucleotide in the cytoplasm, or in a tRNA-bound form. On the other hand, KR has been shown to exert growth inhibitory effects and also induce apoptosis. It has been implicated in the reduction of intracellular ATP level and mitochondrial membrane potential and the induction of reactive oxygen species, whereas CK protects against mitochondrial disruption and apoptosis in HL-60 cells. In addition, treatment with KR leads to cytotoxic effects on mouse, human, and plant tumor cells. Thus, iPA and KR appear to have an important role in the induction of cell death in different types of cancer cells.

Therefore, In the present work, we report our results from a study designed to determine the time dose-dependent antiproliferative and cytotoxicity effect of iPA and KR against on MCF-7 breast cancer and HCT-15 colon cancer cell lines that measured by the SRB assay and other antiproliferation assays. Also incubation of the MCF-7 and HCT-15 cell lines with different concentrations of iPA and KR investigated after treatment with significant morphological changes including cell rounding and detachment from the substratum. Then dose-dependent cell cycle arrest and apoptogenic effect of iPA and KR on cell lines were investigated. As a complementary information related to the antiproliferative activity, iPA interaction with DNA has been studied analyzing absorbance changes in the UV–vis frequency range with the aim to obtain structural information regarding the iPA binding mode, apparent binding constant, and the effects of iPA complexation on the biopolymer secondary structure. Additionally, we present results obtained from the interaction of iPA and BSA since protein–drug binding greatly influences absorption, distribution, metabolism, and excretion properties of typical drugs, studies on the protein–drug binding are important for the elucidation of the reaction mechanisms, providing a pathway to the pharmacokinetics and pharmacodynamic mechanisms of these substances in various tissues.

4. MATERIALS AND METHODS

4.1 Chemicals and materials

iPA and KR dissolved in DMSO was from Sigma company. Trypsin, Trypan Blue, antibiotic and antimycotic agent, fetal bovine serum (FBS), SRB, DMSO, and fish sperm DNA (fs-DNA), Bovine Serum Albumin, Kinetin Riboside were purchased from Sigma Chemical Co. (St. Louis, MO). Chemicals and solvents for iPA synthesis were purchased from Sigma-Aldrich Italia (Milan, Italy).

4.2 Chemical synthesis of iPA

iPA was prepared following the method described by Robins [115]. Briefly, reaction of adenosine with isopentenyl bromide affords iPA in 40% overall yield. An alternative procedure required more expensive 6-chloropurine riboside and isopentenylamine, but proceded with 82% yield of the final product.

4.3 Cell culture

Human breast cancer MCF-7 and HCT-15 colon cancer cells were supplied from ATCC and were maintained in the standard medium and grown as a monolayer in Dulbecco's Modified Eagle Medium (DMEM) containing 10% FBS), 2 mM glutamine, 100 units/ml penicillin, and 100 µg/ml streptomycin. Cultures were maintained at 37 °C with 5% CO_2 in a humidified atmosphere.

4.4 *In vitro* evaluation of cytotoxic activities by SRB assay

Growth activity of iPA and KR *in vitro* were evaluated by the SRB assay [116-117]. iPA and KR stock solution (10 mM in DMSO) was stored at 4°C and diluted with DMEM up to 0.1–1 mM range at room temperature before treatment. The final percentage of DMSO in the reaction mixture was less than 1% (v/v). Cancer cells (2×10^3 cells/ well) were plated in 96-wells plates and incubated in medium for 24 hours. Serial dilutions of individual compounds were added. The plates were incubated at 37 °C, for 72 hours prior to addition of iPA and KR. The assay was terminated by the addition of 50 µL of ice-cold trichloroacetic acid (final concentration, 10% TCA) and incubated for 60 min at 4°C. The plates were washed five times with distilled water and air-dried. SRB solution (50 µL) at 0.4% (w/v) in 1% acetic acid was added to each of the wells, and plates were incubated for 30 min at room temperature. The residual dye was removed by washing five times with 1% acetic acid. The plates were air-dried or under hood. Bound stain was subsequently eluted with 10 mM Trizma base, and the absorbance was read on an ELISA plate reader at a wavelength of 540 nm and used as a relative measure of viable cell number. The percentage of growth inhibition was calculated by using the equation: percentage growth inhibition $(1- A_t/A_c) \times 100$, where At and Ac represent the absorbance in treated and control cultures, respectively. IC_{50} was determined by interpolation from dose–response curves.

4.5 In vitro evaluation of cytotoxic activities by MTT assay

MTT is a simple colorimetric assay, as a test for cell proliferation and survival, has been adapted for theVmeasurement of cytotoxicity. This assay involves the ability of viable cells to convert a soluble tetrazolium salt MTT (3-(4,5-dimethylthiazol-2-yl)-2,5-diphenyl tetrazolium bromide) into a blue formazan endproduct by mitochondrial dehydrogenase enzymes. The blue color reaction is used as a measure of cell viability. The assay is performed in 96-well plates, and results are read on a multiwell spectrophotometer. For this purpose, 2×10^3 cells in 150 μL of culture medium were seeded in each well of 96 wells. The assay was run in quadruplicate so that control and dilution values were obtained as the mean values of four identical wells. After 24 h incubation at 37°C under a humidified 5% CO_2 containing air atmosphere, the series of drug concentrations were prepared and added to each well. After 72 hours incubation 25 μL of 5 mg/ml of MTT (Sigma Chemical Co.) in saline was added into each well and incubated for a further 4 hours at 37°C and then removed and formazan precipitate. 200 μM of DMSO was added to each well for solubilization of precipitated formazan. The absorbance was read on an ELISA plate reader at a wavelength of 540 nm and used as a relative measure of viable cell number. The percentage of growth inhibition was calculated by using the equation: percentage growth inhibition $(1- A_t/A_c) \times 100$, where At and Ac represent the absorbance in treated and control cultures, respectively. IC_{50} was determined by interpolation from dose–response curves.

4.6 Tryptan blue exclusion test

The trypan blue exclusion test is used to determine the number of viable cells present in a cell suspension. In fact programmed cell death or apoptotic cell death was confirmed by trypan blue was analyzed by trypan blue dye (Sigma–Aldrich, Germany) on both HCT-15 and MCF-7 cell line. The cell culture plates with 70–80% confluence were treated with IC50 dose of iPA and KR for 24 h, 48h and 72hr. The supernatant medium with floating cells was collected after treatment and centrifuged to collect the dead and apoptotic cells. The cell pellet was resuspended in serum free media. Equal amounts of cell suspension and trypan blue were mixed and this was analyzed under a microscope. The cells which were viable excluded the dye and were colorless and the ones whose cell membrane was destroyed were turning into blue. If the proportion of colorless cells were more compared to the ones that were colored then the death can be characterized as apoptotic.

4.7 Evaluation of cell morphology

It is now generally accepted that cell death is an important phenomenon, reflected by the appearance of numerous publications on the subject every year. For more than 150 years, morphological features played the leading role in the description of cell death [118]. However, during the past three decades cell death has been characterized on the molecular level, which markedly increased our understanding

of the morphology [119]. Under inverted microscope, cell shape and its changes can be observed clearly. Treated and untreated (control) cells were viewed using an inverted phase-contrast microscope model Zeiss and photographed using a Nikon camera attached to the microscope. The evaluation of cell morphology investigated by the incubation of the cells with different concentrations of iPA and KR after 48 h treatment. HCT-15 and MCF-7 cells were plated at about 20,000 cells/well on chamber-slides (8 wells), were treated with 0, 2.5, 5 and 10μM of iPA for 48 hours. After rinsing in PBS, cells were either fixed in methanol and stained with 10% Giemsa and photographed using a Nikon camera attached to the microscope.

4.8 Cell cycle analysis by flowcytometery

Analysis of a population of cells replication state can be achieved fluorescence labelling of the nuclei of cells in suspension and then analyzing the fluorescence properties of each cell in the population. Quiescent and G_1 cells will one copy of DNA and will therefore have 1X fluorescence intensity. Cells in G_2/M phase of cell cycle will have to copies of DNA and accordingly will have 2X intensity. Since the cells in S phase are synthesizing DNA they will have fluorescence values between the 1X and 2X populations. The resulting histograms consists of three populations: two peaks (G_1 and G_2/M populations) and the S-phase population.

Apoptosis and cell cycle profile were assessed by flow cytometry analysis by DNA staining with propidium iodide (PI). MCF-7 and HCT-15 cells were plated at a density of 5 x 10^5 cells/well on six-well plates. Cells treated with iPA at different concentration of 1, 5 and 10 μM for 72 hours were harvested, rinsed in PBS, suspended in 600μl of PBS containing 1%FBS, fixed by 1.4 ml 80% ethanol and stored at -20 °C in fixation buffer. Then the pellets were suspended in 1 ml of fluorochromic solution [0.08 mg/ml PI in 1x PBS] at room temperature in the dark for 60 min. The DNA content was analyzed by FACScan flow cytometer (Beckman Counter, cytomics FC 500) and CellQuest software (Becton Dickinson). The population of apoptotic nuclei (subdiploid DNA peak in the DNA fluorescence histogram) was expressed as the percentage in the entire population.

4.9 DNA Fragmentation Analysis

Cells were harvested, washed with ice-cold Phosphate Buffer Salin (PBS), and lysed in 50mL lysis buffer (5mM Tris–HCl pH 8.0, 10mM EDTA, and 0.5% Triton X-100) on ice for 20 min. Then, the cell lysate was centrifuged at 12 000 rpm for 20 min. The supernatant was treated with RNase A (100 mg/mL) at 378C for 60 min and proteinase K (200 mg/mL) at 508C for 120 min. Then, the DNA was extracted by phenol/chloroform before loading and analysis by 1.8% agarose gel electrophoresis. The gels were run at 50V for 120 min in Tris–borate/EDTA (TBE) buffer. Approximately, 20 mL DNA was loaded, stained by ethidium bromide, and visualized under UV light.

4.10 Clonogenic assays

Clonogenic assay or colony formation assay is an *in vitro* cell survival assay base on the ability of single cell to grow an colony. The colony is defined to consist of at least 50 cells. The assay essentially tests every cell in the population for its ability to undergo "unlimited" division. Clonogenic assay is the method of choice to determine cell reproductive death after treatment with ionizing radiation, but can also be used to determined effectiveness of other cytotoxic agents. Only a fraction of seeded cell retains the capacity to product colonies.

MCF-7 and HCT-15 cells/well were seeded in 6-well tissue culture plates at a density of 500-700 cells/well according to the morphology and growth patterns of each cell line and were allowed adhere for 24 hours before treatment. The cells were treated with different concentration of iPA and KR for 12 days. Triplicate samples were used for each treatment. Medium containing the treatment was replaced with a drug-free medium after the indicated time points. Plates were rinsed in PBS and colonies were methanol-fixed and stained with 10% Giemsa and Clones were counted under a light microscope.

4.11 DNA titration experiments

The absorbance at 260 and 280 nm was recorded, in order to check the protein content of DNA solution. DNA (5 mg/ml) was dissolved in distilled water (pH 7) at 4°C for 24 h with occasional stirring to ensure the formation of a homogeneous solution. The final concentration of the DNA solution was determined spectrophotometrically at 260 nm using molar extinction coefficient ε_{260} = 6600 cm^{-1} M^{-1} (expressed as molarity of phosphate groups). The UV absorbance at 260 nm of a diluted solution (1/187.5) of DNA used in our experiments was 0.666 and the final concentration of the DNA solution was 12.5 mM in DNA. The appropriate amounts of iPA and KR (0.05–12.5 mM) were prepared in distilled water and added dropwise to DNA solution in order to attain the desired ligand/DNA molar ratios (r) of 1/40, 1/20, 1/10, 1/5, 1/2 and 1 with a final DNA concentration of 6.25 mM. The pH of the solutions was adjusted at 7.0 ± 0.2 using NaOH solution.

4.12 BSA binding experiments

BSA stock solution 2.5 x 10^{-5} $molL^{-1}$ (MW= 68000 g/mol) was prepared in working solution 0.05 $molL^{-1}$ Tris-HCl buffer Ph=7.4 containing 0.1 mol L^{-1} NaCl then stored at 4° C. The solutions of drugs 1.5 x 10^{-5}- 25 x 10^{-5} $molL^{-1}$ were prepared by dissolving the drug in working solution 0.05 $molL^{-1}$ Tris-HCl buffer pH=7.4 containing 0.1 mol L^{-1} NaCl. In the final step, drug solution was added dropwise to the protein solution with constant stirring to ensure the formation of homogeneous solution and to attain the desired drug. The pH of the solution was adjusted to 6.8-7.4 by the addition of NaOH/NaOD or HCl/DCl (0.1 M).

5. RESULTS

5.1 Antiproliferation evaluation

5.1.1 Inhibition growth of iPA against MCF-7

Antiproliferation activity of iPA against human breast cancer MCF-7 cells was investigated by SRB assay and results showed that iPA inhibits the growth of MCF-7 in a dose dependent manner with an IC_{50} value of 12.2 µmol/L. In the presence of different concentrations of iPA, the cells were inhibited ranging from 10% to 90% of viable cells (Figure 5.1A). iPA inhibited the proliferation of MCF-7 cells in a concentration and time-dependent manner. iPA caused dose dependent cell death in MCF-7. From these two data we have calculated an IC_{50} of 12.2 µmol/L (Figure 5.1B).

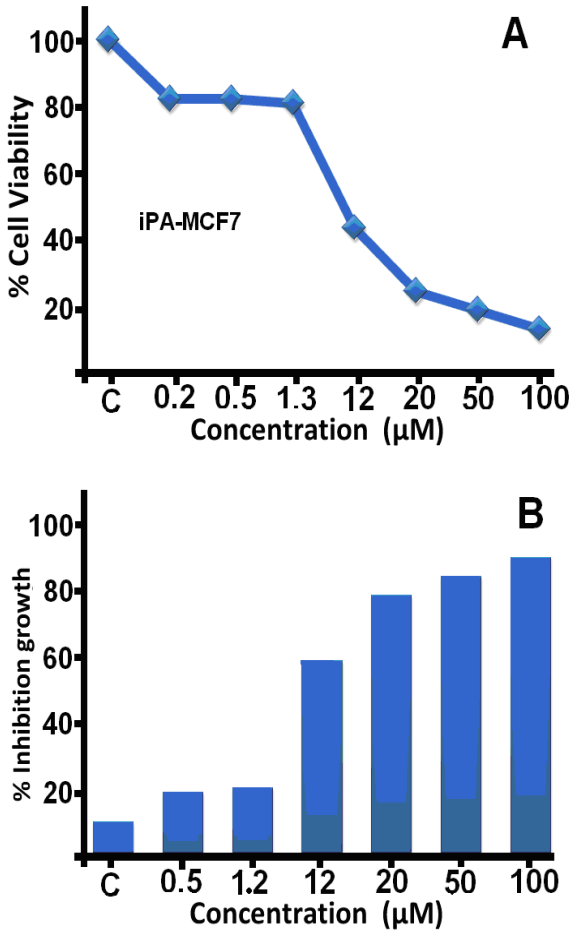

Figure 5.1. (A) Effects of iPA on the proliferation of MCF-7*. Dose of compound required to inhibit cell growth by 50% compared to untreated cell controls. All experiments were carried out in triplicate wells and each*

experiment was repeated twice. ***(B) Inhibition growth of of iPA on MCF-7.*** *The percentage of growth inhibition was calculated by using the equation: (1-A_t/A_c) x 100, where A_t and A_c represent the absorbance in treated and control cultures, respectively. IC_{50} was determined by interpolation from dose–response curves.*

5.1.2 Inhibition growth of iPA against HCT-15

Treatment with iPA inhibits the growth of human colon cancer HCT-15 cells in a dose dependent manner with an IC_{50} value of 2.5 µmol/L. In the presence of different concentrations of iPA, the cells were inhibited ranging from 10% to 90% of viable cells (Figure 5.2A). iPA caused dose dependent cell death in HCT-15. From these two data we have calculated as IC_{50} of 2.5 µmol/L (Figure 5.2B).

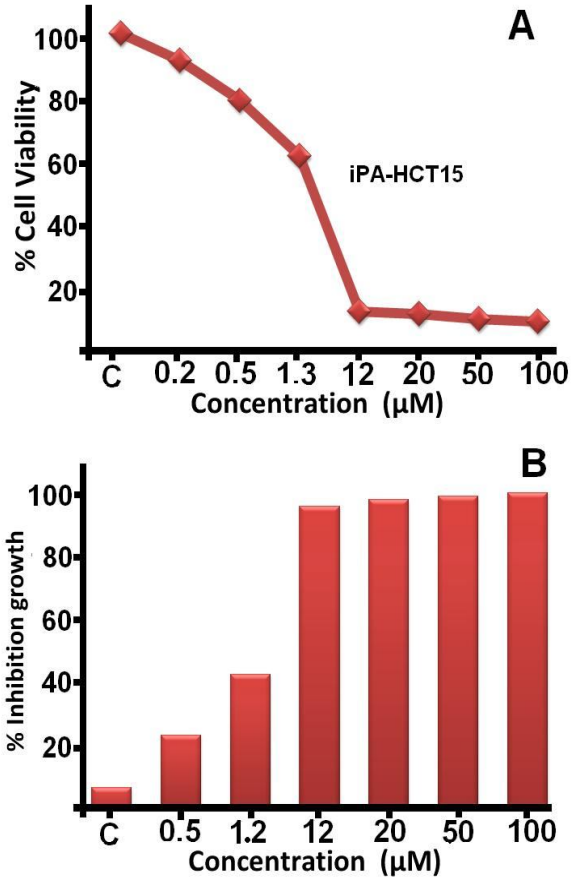

Figure 5.2. (A) Effects of iPA on the proliferation of HCT-15*. Dose of compound required to inhibit cell growth by 50% compared to untreated cell controls. All experiments were carried out in triplicate wells and each experiment was repeated twice.* ***(B) Inhibition growth of of iPA on HCT-15.*** *The percentage of growth inhibition was calculated by using the equation: (1-*

A_t/A_c) x 100, where A_t and A_c represent the absorbance in treated and control cultures, respectively. IC_{50} was determined by interpolation from dose–response curves.

5.1.3 Inhibition growth of KR against MCF-7

KR was evaluated for its growth inhibitory effect on MCF-7 breast cancer cell line. Therefore the cells were treated with KR at different concentrations, ranging from 1 μM to 500 μM for 4 days (Figure 5.3.). The results from Figure 5.3. show that activity of KR started before first day since there is distance between points in first day, since we expected that points should be close to eachothers at first day, so decided to reaped the experiment again and read absorbances after hours, not after days. So the cells were treated with KR at different concentrations, ranging from 1 μM to 100 μM for 86 hours (Figure 5.4) and absorbances at 540 nm were read after 6, 12, 28, 52 and 86 hours.

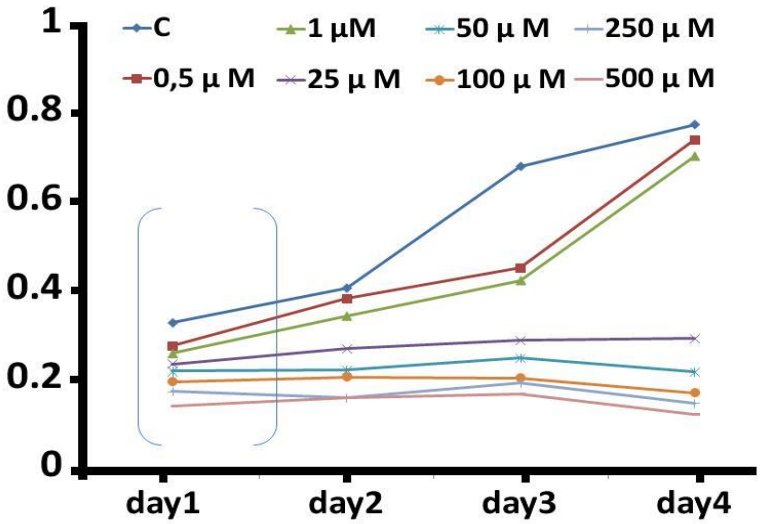

Figure 5.3. *Antiproliferative effect of KR on MCF-7. Proliferation index was evaluated by the SRB assay in cancer cell lines with ranging from 1μM to 500 μM for 4 days. The values are the mean of three independent experiments.*

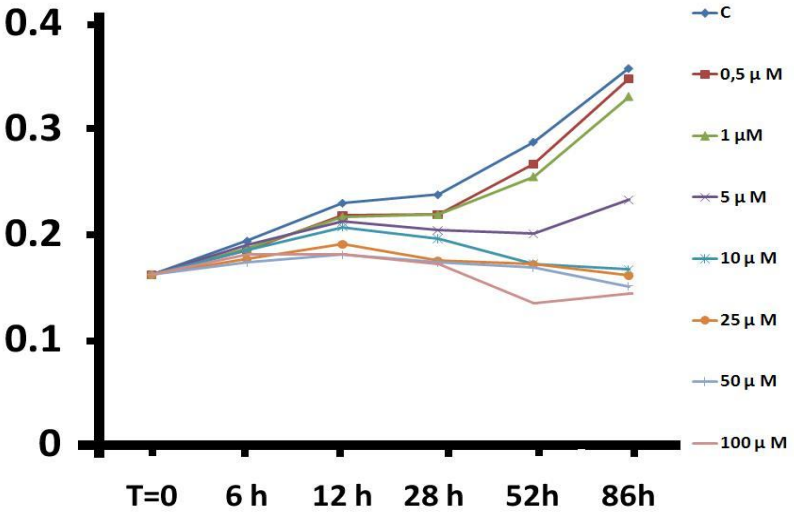

Figure 5.4. *Antiproliferative effect of KR on MCF-7. Proliferation index was evaluated by the SRB assay in cancer cell lines with ranging from 1µM to 100 µM for 86 hours. absorbances at 540 nm were read after 6, 12, 28, 52, 86 hours.The values are the mean of three independent experiments.*

The compound concentration causing a 50% cell growth inhibition (IC_{50}) was determined by interpolation from dose–response curves. The percentage growth inhibition was calculated by comparison of the absorbance of treated versus control cells. The antiproliferative effects mediated by KR on the growth of MCF-7 cell lines, was monitored for a total of four days. From these two data we have calculated as IC_{50} of 15 µmol/L (Figure 5.5).

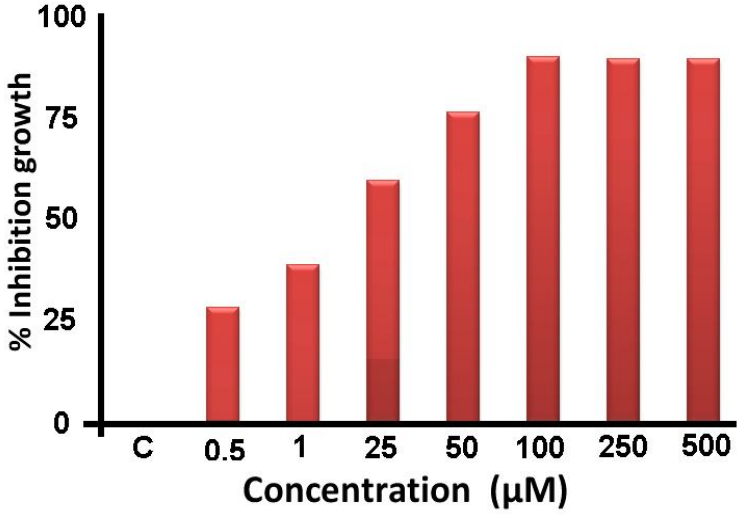

Figure 5.5. *Inhibition growth of of KR on MCF-7. The percentage of growth inhibition was calculated by using the equation: (1- A_t/A_c) x 100, where A_t and A_c represent the absorbance in treated and control cultures, respectively. IC_{50} was determined by interpolation from dose–response curves.*

5.1.4 Inhibition growth of KR against HCT-15

Kinetin riboside was evaluated for its growth inhibitory effect on HCT-15 colon cancer cell line. Therefore the cells were treated with KR at different concentrations, ranging from 1 µM to 500 µM for 4 days (Figure 5.6).

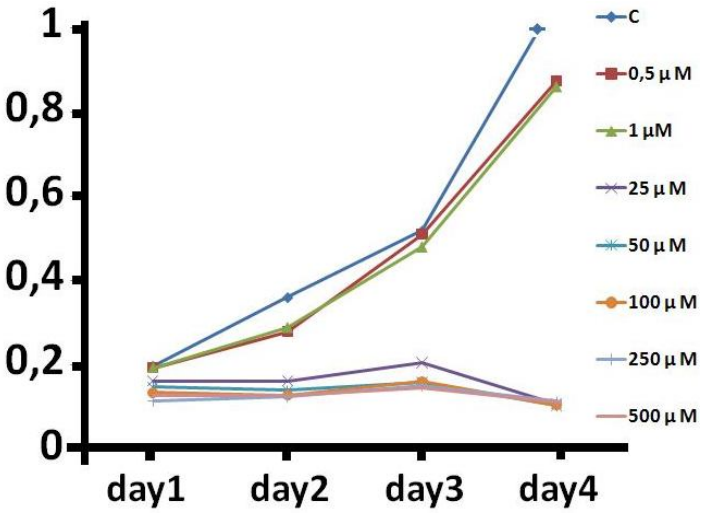

Figure 5.6. *Antiproliferative effect of KR on HCT-15. Proliferation index was evaluated by the SRB assay in cancer cell lines with ranging from 1µM to 500 µM for 4 days. The values are the mean of three independent experiments.*

In the presence of different concentrations of KR, the cells were inhibited ranging from 10% to 90% of viable cells (Figure 5.7). KR inhibited the proliferation of HCT-15 cells in a concentration and time-dependent manner. KR caused dose dependent cell death in HCT-15. From these two data we have calculated as IC_{50} of 2.5 µmol/L (Figure 5.7).

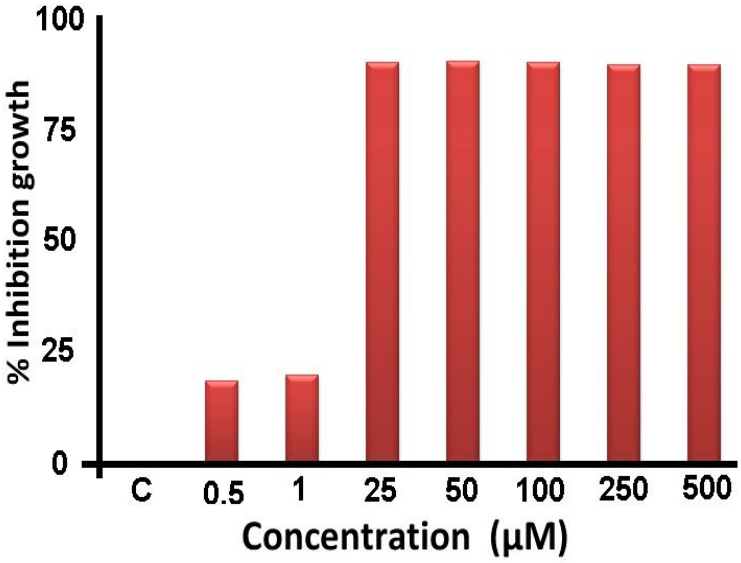

Figure 5.7. *Inhibition growth of of KR on HCT-15. The percentage of growth inhibition was calculated by using the equation: (1- A_t/A_c) x 100, where A_t and A_c represent the absorbance in treated and control cultures, respectively. IC_{50} was determined by interpolation from dose–response curves.*

5.2 Cell shape and morphology study

Cell death occurs frequently in complex, multicellular, organisms to maintain tissue homeostasis. For example, cells die during embryonic development. Also, the killing of infected cells by cytolytic effector cells of the immune system is an example of cell death in tissue maintenance. It is now generally accepted that cell death is an important phenomenon, reflected by the appearance of numerous publications on the subject every year. For more than 150 years, morphological features played the leading role in the description of cell death. However, during the past three decades cell death has been characterized on the molecular level, which markedly increased our understanding of the morphology.

Cell shape and morphology of treated and untreated (control) cells were viewed using an inverted phase-contrast microscope model Zeiss and photographed using a Nikon camera attached to the microscope. Bellows figures show the incubation of the cells with different concentrations of iPA and KR after 72 hours treatment. Control group showed regular polygonal shape and cell antennas were short. The cell morphology of treated cells was affected by iPA and KR treatment and loss of adhesion, rounding, cell shrinkage and detachment from the substratum (Figure 5.8, 5.9, 5.10, 5.11).

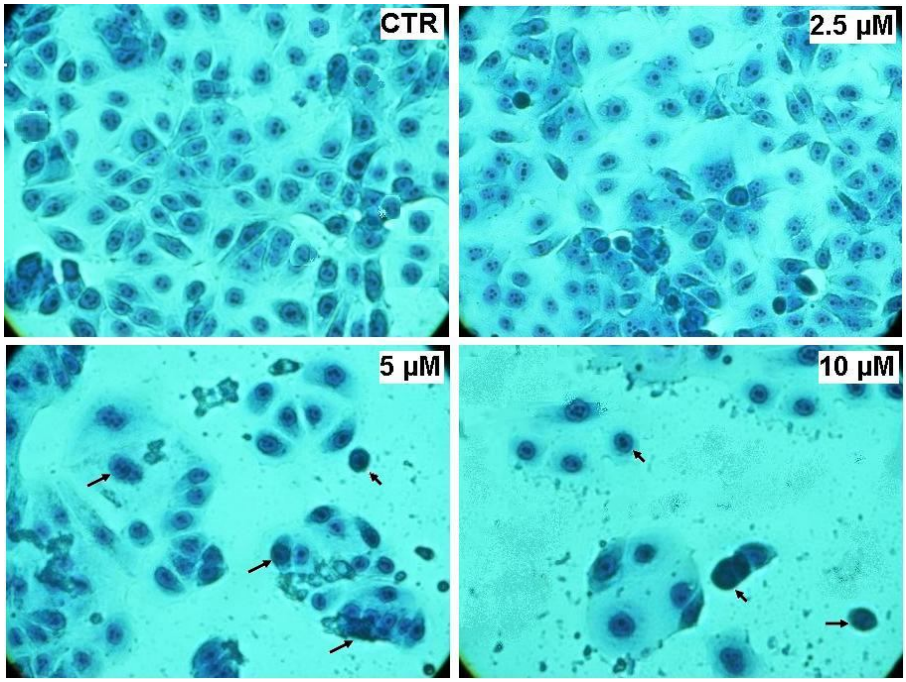

Figure 5.8. *Changes in cell morphology and iPA treatment of MCF-7 cells*

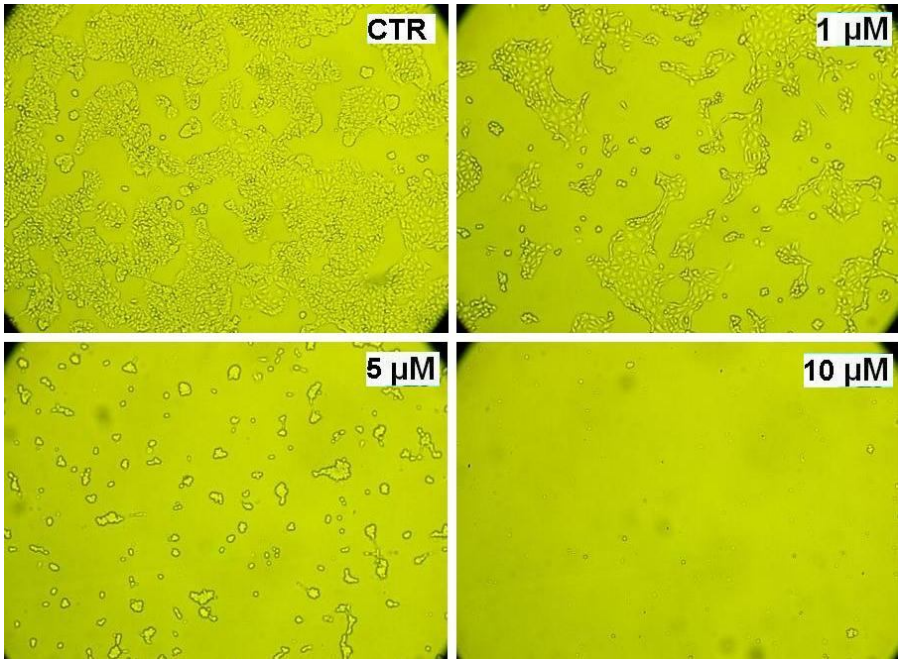

Figure 5.9. *Changes in cell morphology and iPA treatment of HCT-15 cells*

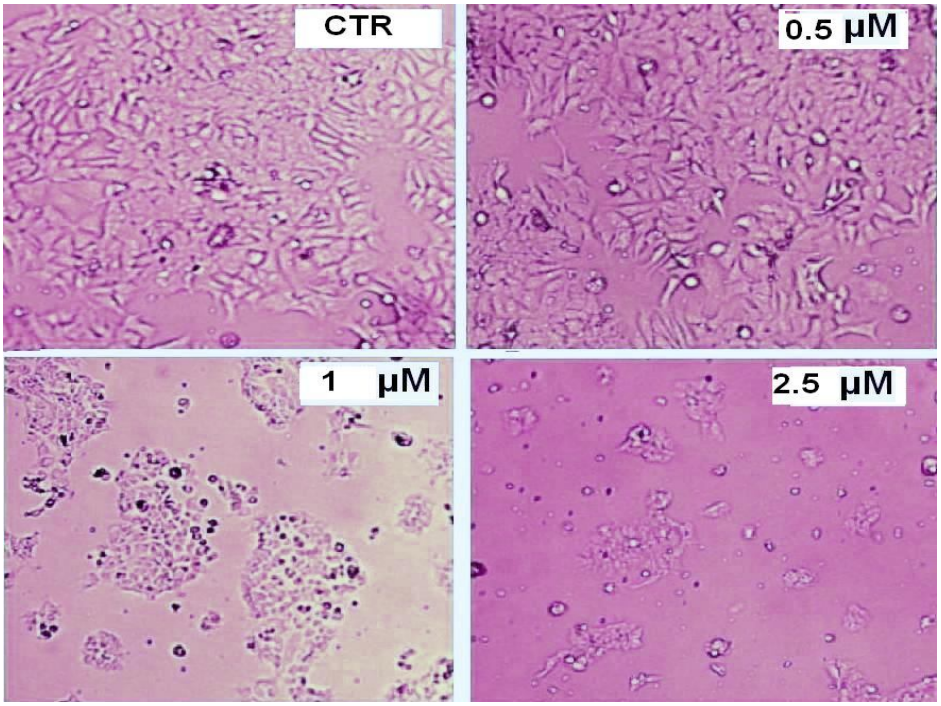

Figure 5.10. *Changes in cell morphology and KR treatment of HCT-15 cells*

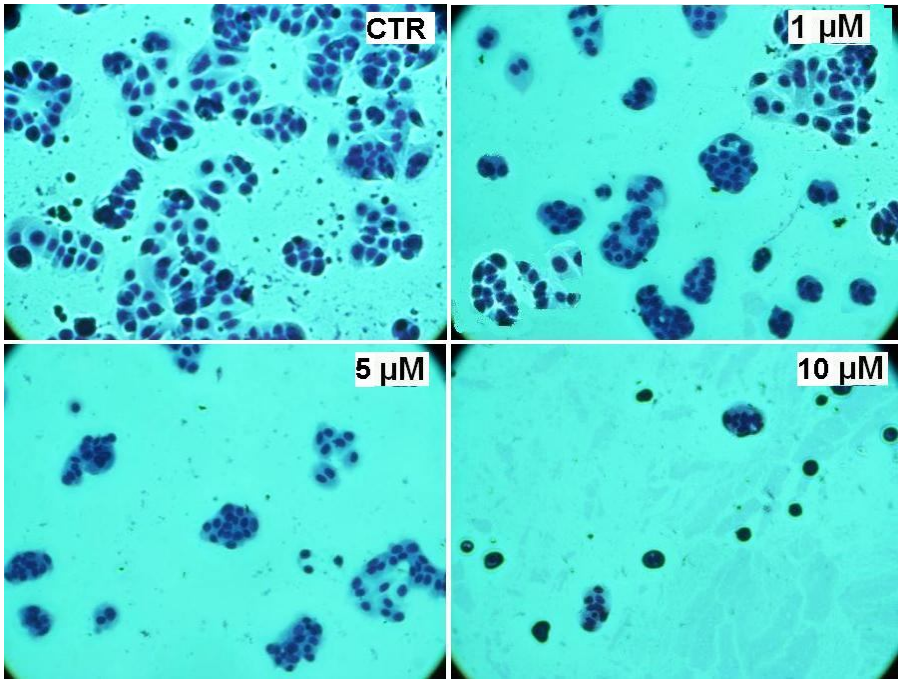

Figure 5.11. *Changes in cell morphology and KR treatment of MCF-7 cells*

5.3 Cell Cycle Analysis

5.3.1 Cell Cycle

The cell cycle, or cell-division cycle, is the series of events that takes place in a cell leading to its division and duplication (replication). In cells without a nucleus (prokaryotic), the cell cycle occurs via a process termed binary fission. In cells with a nucleus (eukaryotes), the cell cycle can be divided in two brief periods: interphase-during which the cell grows, accumulating nutrients needed for mitosis and duplicating its DNA-and the mitosis (M) phase, during which the cell splits itself into two distinct cells, often called "daughter cells". The cell-division cycle is a vital process by which a single-celled fertilized egg develops into a mature organism, as well as the process by which hair, skin, blood cells, and some internal organs are renewed. The cell cycle consists of four distinct phases: G_1 phase, S phase (synthesis), G_2 phase (collectively known as interphase) and M phase (mitosis). M phase is itself composed of two tightly coupled processes: mitosis, in which the cell's chromosomes are divided between the two daughter cells, and cytokinesis, in which the cell's cytoplasm divides in half forming distinct cells. Activation of each phase is dependent on the proper progression and completion of the previous one. Cells that have temporarily or reversibly stopped dividing are said to have entered a state of quiescence called G_0 phase (Figure 5.12).

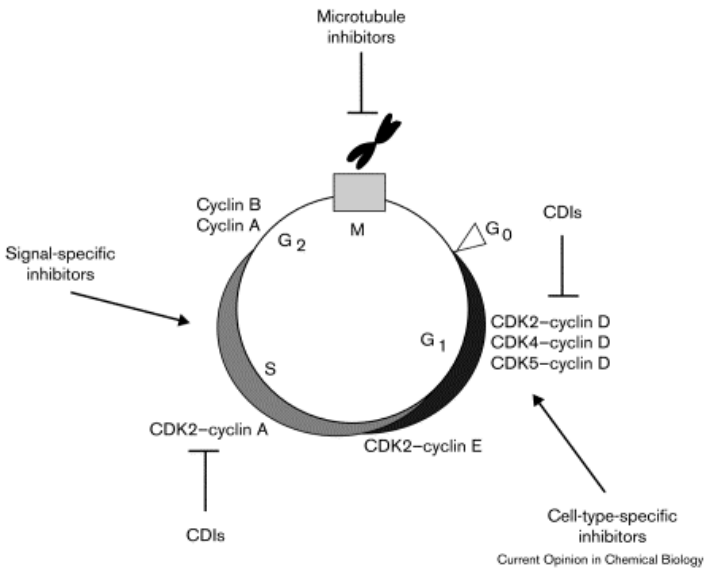

Figure 5.12. *The eukaryotic cell cycle is divided into four distinctphases (G1, S, G2, M), each of which is regulated by a series of proteins that are attractive targets for small molecule cell-cycle inhibitors.*

5.3.2 Flow cytometry (FCM)

FCM is a technique for counting and examining microscopic particles, such as cells and chromosomes, by suspending them in a stream of fluid and passing them by an electronic detection apparatus. It allows simultaneous multiparametric analysis of the physical and/or chemical characteristics of up to thousands of particles per second. FCM is routinely used in the diagnosis of health disorders, especially blood cancers, but has many other applications in both research and clinical practice. Fluorescence-activated cell sorting (FACS) is a specialized type of flow cytometry. It provides a method for sorting a heterogeneous mixture of biological cells into two or more containers, one cell at a time, based upon the specific light scattering and fluorescent characteristics of each cell. Two of the most popular flow cytometric applications are the measurement of cellular DNA content and the analysis of the cell cycle.

5.3.3 Measurement of cellular DNA content and cell cycle by FACS

The nuclear DNA content of a cell can be quantitatively measured at high speed by flowcytometry. Initially, a fluorescent dye that binds stoichiometrically to the DNA is added to a suspension of permeabilized single cells or nuclei. The principle is that the stained material has incorporated an amount of dye proportional to the amount of DNA. The stained material is then measured in the flow cytometer and the emitted fluorescent signal yields an electronic pulse with a height (amplitude) proportional to the total fluorescence emission from the cell. Thereafter, such fluorescence data are considered a measurement of the cellular DNA content. Samples should be analyzed at rates below 1000 cells per second in order to yield a good signal of discrimination between singlets or doublets. Since the data obtained is not a direct measure of cellular DNA content, reference cells with various amounts of DNA should be included in order to identify the position of the cells with the normal diploid amount of DNA. Some of the common reference cells often used for DNA measurements are human leukocytes or red blood cells from chicken and trout . Commonly DNA measurements are expressed as a DNA index of the ratio of sample DNA peak channel to reference DNA peak channel. In addition to determining the relative cellular DNA content, flow cytometry also enables the identification of the cell distribution during the various phases of the cell cycle. Four distinct phases could be recognized in a proliferating cell population: the G_1, S (DNA synthesis phase), G_2 and M-phase (mitosis). However, G_2 and M-phase, which both have an identical DNA content could not be discriminated based on their differences in DNA content. Diverse software containing mathematical models that fit the DNA histogram of a singlet have been developed in order to calculate the percentages of cells occupying the different phases of the cell cycle.

5.3.4 Apoptosis

Apoptosis is the process of programmed cell death through a tightly controlled program that plays important roles in many normal processes, ranging from fetal development to adult tissue homeostasis [120]. During apoptosis, the nucleus and cytoplasm condense to produce membrane-bound apoptotic bodies that are phagocytosed by macrophages or adjacent cells. A tumor is a disease state characterized by uncontrolled proliferation and a loss of apoptosis. Compounds that block or suppress the proliferation of tumor cells by inducing apoptosis are considered to have potential as antitumor agents [121].

5.3.5 MCF-7 cell cycle analysing in treatment with iPA

To study the mechanism of antiproliferative activity by iPA in detail, we analyzed the effects of Ipa treatment on cell cycle distributions of MCF-7 cells. Cells were treated with various concentration of iPA for 72 h and subject to FACS analysis after PI staining of the chromosomal DNA.

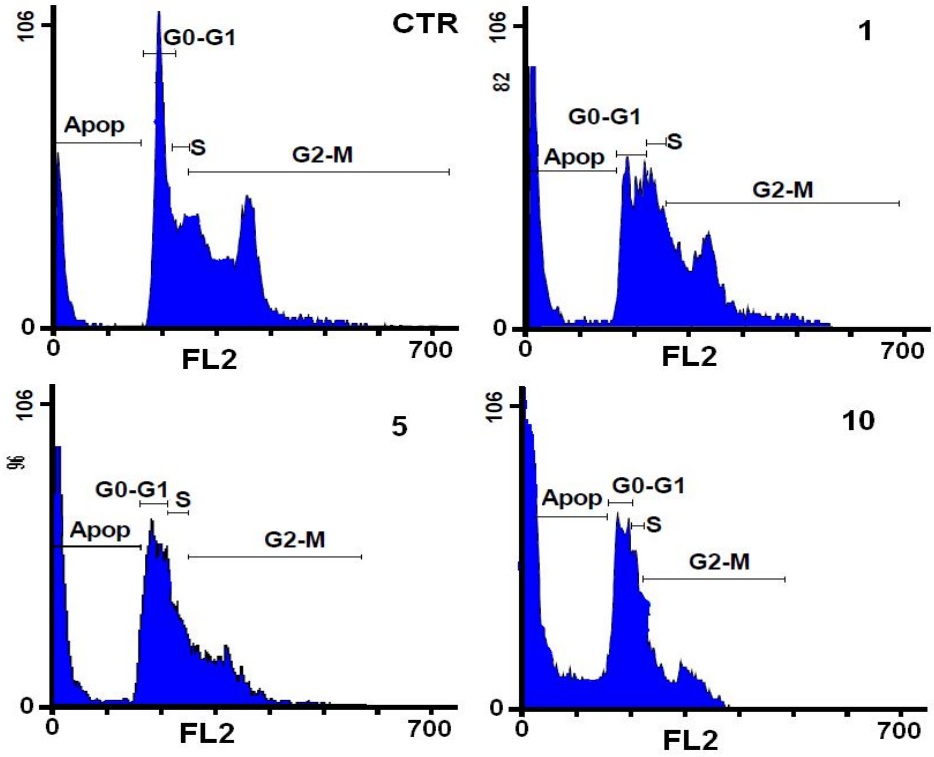

Figure 5.13. *Flow cytometric analysis of MCF-7 cells. Values are expressed as percentage of the cell population in the G_1, S, and G_1/M phase of cell cycle.*

In histograms of FACS analysis, untreated proliferative MCF-7 cells showed cell cycle distributions of 25.99% in G_1/G_0, 11.14% in S, 52.38% in G_2/M, and 12.27% in sub G_1/G_0 phase. At all concentrations, iPA leads to decrease in the percentage of cells in G_2/M phase, which and increase percentage of cells in sub G_1/G_0 phase. At 10μM of iPA, these populations reached 23.95% for G_2/M and 40.66 μM for sub G_1/G_0 phase (Figure. 5.13 and 5.14). These data indicates that iPA has an activity to arrest MCF-7 cell growth in G_2/M.
In addition, cell cycle analysis was performed, and it was found that the drug addition did not good change the duration of the cell cycle in S and G_0/G_1 phases but as shown in Figure. 5.13 and 5.14 in treatment of MCF-7 cells to 10μM of iPA was found to induce apoptosis approximately 40.66 %.

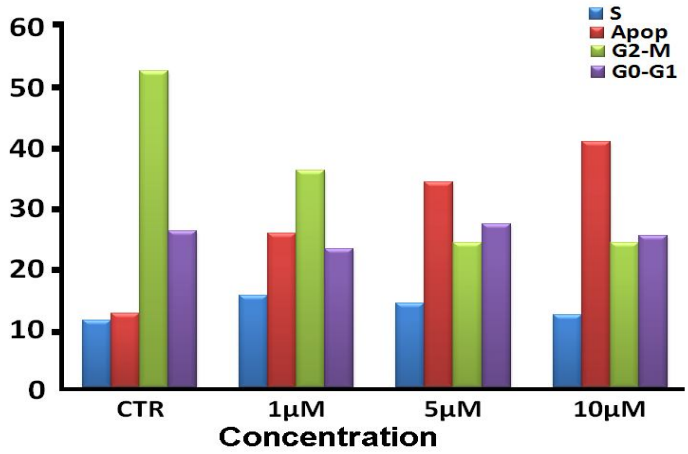

Figure 5.14. Cell cycle analysis of MCF-7 cells treated with 0, 1, 5, 10μM of iPA.

5.3.6 HCT-15 cell cycle analysing in treatment with KR

To study the mechanism of antiproliferative activity by KR in detail, we analyzed the effects of Ipa treatment on cell cycle distributions of HCT-15 cells. Cells were treated with various concentration of KR for 72 h and subject to FACS analysis after PI staining of the chromosomal DNA. In histograms of FACS analysis, untreated proliferative HCT-15 cells showed cell cycle distributions of 68.25% in G_1/G_0, 8.68% in S, 14.54% in G_2/M, and 4.11% in sub G_1/G_0 phase. At the concentration of 5 μM, KR leads to decrease in the percentage of cells in G0/G1 phase, which and increase percentage of cells in S and G_2/M phase. At 5μM of KR, these populations reached 33.3% for G_2/M and 16.65% for S phase and 47.78% for 33.3% for G_0/G_1(Figure. 5.15. and 5.16.). These data indicates that KR has an activity to arrest HCT-15 cell growth in G_2/M and G_0/G_1. In addition, cell cycle analysis was performed, and it was found that the drug addition did not change the duration of the cell cycle in sub G_1/G_0 phase as shown in Figure. 5.15 and 5.16.

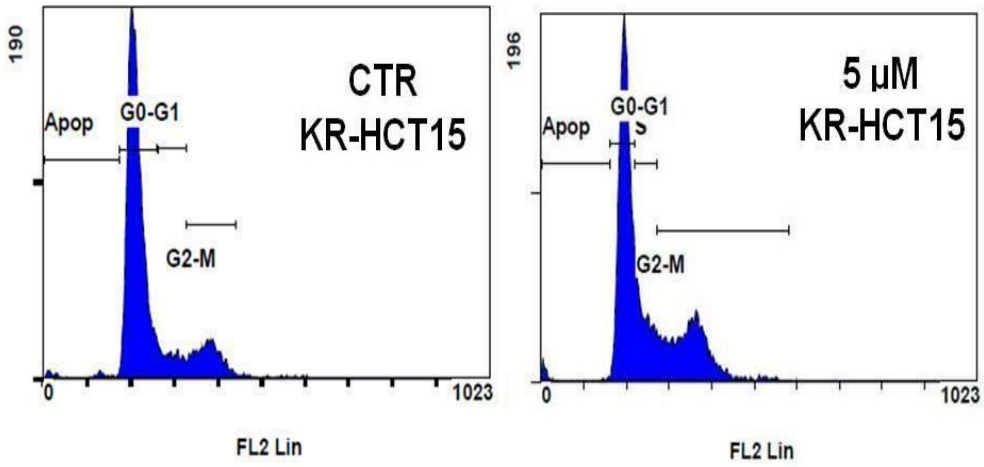

Figure 5.15. *Flow cytometric analysis of HCT-15 cells. Values are expressed as percentage of the cell population in the G_1, S, and G_1/M phase of cell cycle.*

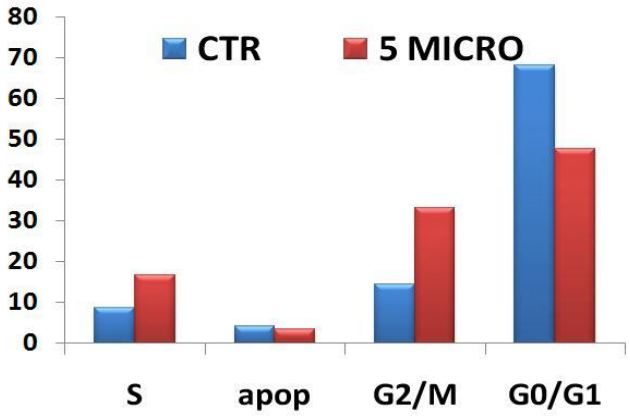

Figure 5.16. *Cell cycle analysis of HCT-15 cells treated with 5 µM of KR.*

5.4 DNA binding study iPA by UV spectroscopy

The UV spectra have been recorded for a constant DNA concentration in different [DNA]/[compound] mixing ratios (*r*). UV spectra of DNA in the presence of a complex derived for diverse (*r*) values are shown representatively for iPA in Figure 5.17. The intrinsic binding constants, *K*, of the compounds with DNA have been determined using the UV spectra of the compounds recorded for a constant concentration in the absence or presence of DNA for diverse (*r*) values. The ntensity at λ_{max}= 259 nm remains almost stable and is accompanied by a red-shift of the λ_{max} up to 269 nm for all complexes (Figure 5.17A).

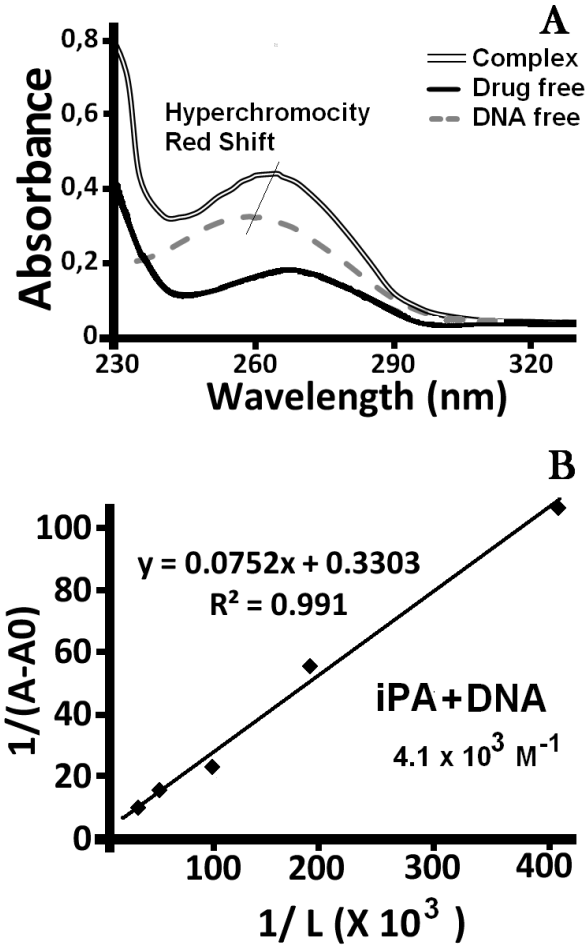

Figure 5.17. *(A) UV-vis absorbance spectra (259 nm) of DNA in the presence of iPA. (B) The plot of 1/(A-A0) vs 1/L for DNA and iPA complexes at different drug concentrations.*

The observed a red-shift of 10 nm from λ_{max} = 258 nm up to 269 nm is an evidence of the stabilization of the DNA duplex [122,123]. The absorption intensity at 258 nm is increased due to the fact that the purine and pyrimidine DNA–bases are exposed because of the binding of the compound to DNA. These characteristics can be attributed to an interaction [124] having caused the changes of the conformation of DNA [125], while the existence of the intercalative binding mode may not be ruled out [126,127]. The observed hyperchromic effect suggests binding to DNA attributed either to external contact (electrostatic or groove binding) or to the fact that iPA could uncoil the helix structure of DNA resulting in a destabilization of the DNA duplex [128]. Any interaction between each compound and FS-DNA could perturb the intraligand centred spectral transition bands of the compound [129]. High significant changes are observed in the position of the π-π* transition bands of

the iPA upon addition of DNA. Our data show that 1/[complexed ligand] almost proportionally increases as a function of 1/[free ligand] (Figure 5.17B.). Therefore, an overall binding constant $K_{iPA–DNA}$=4.4 x 10^3 M^{-1} can be estimated for iPA–DNA.

5.5 BSA binding study iPA by UV spectroscopy

To explore the structural change of BSA by addition of iPA, we measured UV–vis spectra (Figure 5.18) of BSA with various amounts of iPA. BSA free has strong absorbance with a peak at about 278 nm and According to literature [130] the absorption peak at 278 nm appears due to phonyl group of tryptophan residues (Trp) and tyrosines. It can be seen that all the peaks in different iPA concentrations do show considerable shift, however, the intensity is strongly dependant on the iPA concentrations.

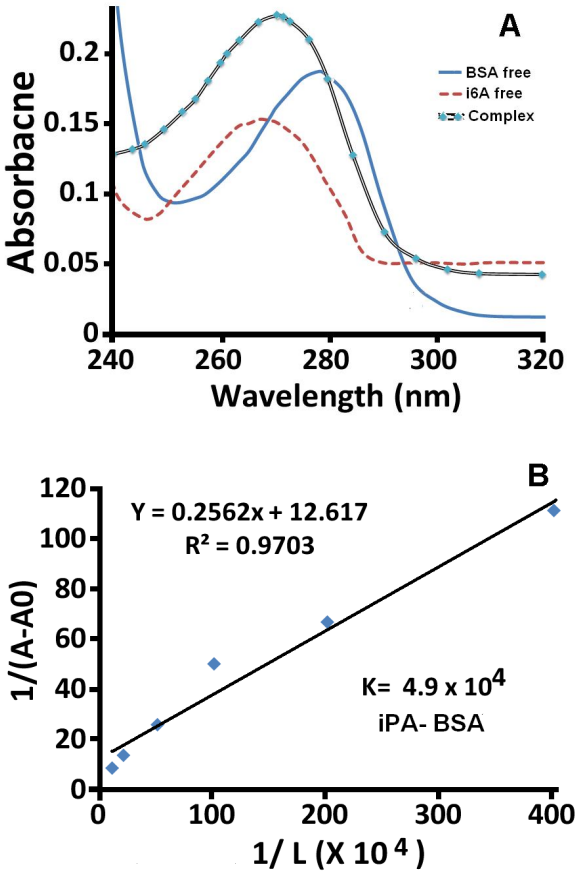

Figure 5.18. *UV–vis absorption spectra of BSA in the presence of 5 at range of 240 nm to 360 nm. The plot of 1/(A-A_0) vs 1/L for BSA-protein and* ***5*** *complexes where A_0 is the initial protein absorption band (278 nm) and A is the recorded absorption at different drug concentrations (L).*

The UV–vis spectra of BSA at different contents of iPA show that in the visible region, the absorption peaks of these solutions showed moderate shifts towards longer wavelength with red shift indicating that with the addition of iPA, the peptide strands of BSA molecules extended more and the hydrophobicity was increased [131]. The spectroscopic results showed that iPA is located along the polypeptide chains with overall affinity constant of K_{iPA}=4.9 x 10^4 M^{-1} and these spectral changes were caused by compound–BSA complex formation, in which compound iPA was strongly bound at the hydrophobic positions of the BSA supported by the hydrophobic interaction. It was obvious that hydrophobic substituents of compound iPA proved to be a key structural unit for their binding abilities to BSA, which might provide some suggestions on the understanding of their exclusive antitumor selectivity against HCT-15 and MCF-7 cell lines.

5.6 Binding Constant study of 5 with DNA and BSA

The ligand–Macromolecules (DNA& BSA) binding constants were determined using UV absorption spectroscopy [132,133]. The calculation of the overall binding constants was carried out on the basis of UV absorption as reported [134]. The equilibrium for ligands and Macromolecules complex can be described as follows:

$$[\text{Macromolecules} + \text{Ligand}] \leftrightarrow [\text{Macromolecules} - \text{Ligand}]K_{ligand}$$
$$K_{ligand} = [\text{Macromolecules} - \text{Ligand}]/ [\text{Macromolecules}][\text{Ligand}]$$

The double reciprocal plot of $1/[A - A_0]$ vs 1/[ligand] is linear and the association binding constant (K) is calculated from the ratio of the intercept on the vertical coordinate axis to the slope [135,136]. Our data of 1/[ligand complexed] almost proportionally increased as a function of 1/[free ligand] and thus the overall binding constants are estimated to be K_{iPA}=4.9 x 10^4 M^{-1} for iPA–BSA and $K_{iPA–DNA}$ =4.4 x 10^3 M^{-1} for iPA–DNA (Figure 5.17B and Figure 5.18B).

6. Conclusions

Antiproliferation activity of iPA and KR against human breast cancer MCF-7 and colon cancer HCT-15 cells were investigated by SRB assay and our results showed that the cytotoxic effect of iPA and KR on cancer cells. iPA and KR caused dose dependent cell death in MCF-7 and HCT-15. We have calculated an IC_{50} of 12.2 µmol/L for iPA against MCF-7 and IC_{50} of 15 µmol/L for KR against MCF-7. Cell shape and morphology of treated and untreated (control) cells were viewed using an inverted phase-contrast microscope model Zeiss and photographed using a Nikon camera attached to the microscope. Control group showed regular polygonal shape and cell antennas were short. The cell morphology of treated cells was affected by iPA and KR treatment and loss of adhesion, rounding, cell shrinkage and detachment from the substratum. The MCF-7 cell cycle analysis by flow cytometry showed that there was a prominent increase in the amount of sub-G_1/G_0 phase by iPA treatment. In histograms of FACS analysis, untreated proliferative MCF-7 cells showed cell cycle distributions of 25.99% in G_1/G_0, 11.14% in S, 52.38% in G_2/M, and 12.27% in sub G_1/G_0 phase. At all concentrations, iPA leads to decrease in the percentage of cells in G_2/M phase, which and increase percentage of cells in sub G_1/G_0 phase. At 10µM of iPA, these populations reached 23.95% for G_2/M and 40.66 µM for sub G_1/G_0 phase. These data indicates that iPA has an activity to arrest MCF-7 cell growth in G_2/M and this increase of hypoploid DNA is an indication of the inhibition of cell growth through a mechanism of apoptosis that has been suggested also for other cell lines. Also untreated proliferative HCT-15 cells showed cell cycle distributions of 68.25% in G_1/G_0, 8.68% in S, 14.54% in G_2/M, and 4.11% in sub G_1/G_0 phase. At the concentration of 5 µM, KR leads to decrease in the percentage of cells in G0/G1 phase, which and increase percentage of cells in S and G_2/M phase. At 5µM of KR, these populations reached 33.3% for G_2/M and 16.65% for S phase and 47.78% for 33.3% for G_0/G_1.These data indicates that KR has an activity to arrest HCT-15 cell growth in G_2/M and G_0/G_1. On the other hand, the connection between DNA damage and apoptosis is supported by a large body of literature [110,111]. At present, no clear evidence of iPA-induced DNA damage has been demonstrated, except the DNA-fragmentation reported by Laezza et al, that is related to iPA treatment of DLD1 colon cancer cells [46,47]. Our result from structural analysis showed interaction of iPA with DNA and the binding constant value ($_{KiPA–DNA}$=4.4 x 10^3 M^{-1}) together with the shift of UV-vis absorbance suggest that iPA interacts at DNA surface [137]. Further research is required in order to demonstrate that this surface-binding effect may be related to DNA damage in MCF-7 cells. Additionally, we present results obtained from the interaction of iPA and BSA since protein–drug binding greatly influences absorption, distribution, metabolism, and excretion properties of typical drugs, studies on the protein–drug binding are important for the elucidation of the reaction mechanisms, providing a pathway to the

pharmacokinetics and pharmacodynamic mechanisms of these substances in various tissues. The spectroscopic results showed that iPA is located along the polypeptide chains with overall affinity constant of $K_{iPA\text{-}BSA}$= 4.9 x 10^4 M^{-1} and these spectral changes were caused by compound–BSA complex formation, in which compound iPA was strongly bound at the hydrophobic positions of the BSA supported by the hydrophobic interaction. It was obvious that hydrophobic substituents of compound iPA proved to be a key structural unit for their binding abilities to BSA, which might provide some suggestions on the understanding of their exclusive antitumor selectivity against HCT-15 and MCF-7 cell lines.

7. References

1. Amasino R: 1955: Kinetin Arrives. The 50th Anniversary of a new plant hormone. Plant Physiol 2005; 138(3): 1177-84.
2. Miller CO, Skoog F, Von Saltza MH, Strong FM: Kinetin, a cell division factor from deoxyribonucleic acid. J Am Chem Soc 1955; 77(5): 1375-81.
3. Mok DW, Mok MC: Cytokinin metabolism and action. Ann Rev Plant Physiol Plant Mol Biol 2001; 52: 89-118.
4. Sakakibara H: Cytokinins: Activity, Biosynthesis, and Translocation. Annu Rev Plant Biol 2006; 57: 431-9.
5. Strnad M: The aromatic cytokinins. Physiol Plant 1997; 101(4): 674-8.
6. Horgan R, Hewett EW, Purse JG, Wareing PF: A new cytokinin from Populus robusta. Tetrahedron Lett 1973; 14(4): 2827-28.
7. Tarkowská D, Dolezal K, Tarkowski P, Astot C, Holub J, Fuksová K, Schmülling T, Sandberg G, Strnad M: Identification of new aromatic cytokinins in Arabidopsis thaliana and Populus x canadensis leaves by LC-(+)ESI-MS and capillary liquid chromatography/frit-fast atom bombardment mass spectrometry. Physiol Plant 2003; 117(4): 579-90.
8. Brzobohatý B, Moore I, Kristoffersen P, Bako L, Campos N, Schell J, Palme K: Release of active cytokinin by a beta-glucosidase localized to the maize root meristem. Science 1993; 262(5136):1051-54.
9. Skoog F, Armstrong DJ, Cherayil JD, Hampel AE, Bock RM: Cytokinin activity: localization in transfer RNA preparations. Science 1966; 154(754): 1354-56.
10. Vreman HJ, Skoog F: Cytokinins in Pisum Transfer Ribonucleic Acid. Plant Physiol 1972; 49(5): 848-51.
11. Vreman HJ, Thomas R, Corse J: Cytokinins in tRNA Obtained from Spinacia oleracea L. Leaves and Isolated Chloroplasts. Plant Physiol. 1978; 61(2): 296-306.
12. Maaß H, Klämbt D: On the biogenesis of cytokinins in roots of Phaseolus vulgaris. Planta 1981; 151(4): 353-8.
13. Inoue T, Higuchi M, Hashimoto Y, Seki M, Kobayashi M, Kato T, Tabata S, Shinozaki K, Kakimoto T: Identification of CRE1 as a cytokinin receptor from Arabidopsis. Nature 2001 22; 409(6823): 1060-63.
14. Mok MC, Martin RC, Dobrev PI, Vanková R, Ho PS, Yonekura-Sakakibara K, Sakakibara H, Mok DW: Topolins and hydroxylated thidiazuron derivatives are substrates of cytokinin O-glucosyltransferase with position specificity related to receptor recognition. Plant Physiol. 2005; 137(3):1057-66.
15. Long AR, Chism GW: The effect of metyrapone on cytokinin ([8-14C]benzylaminopurine) metabolism in mature green tomato pericarp. Biochem Biophys Res Commun. 1987; 144(1):109-14.

16. Barciszewski J, Massino F, Clark BF: Kinetin--a multiactive molecule. Int J Biol Macromol. 2007; 40(3): 182-92.

17. Barciszewski J, Mielcarek M, Stobiecki M, Siboska G, Clark BF: Identification of 6-furfuryladenine (kinetin) in human urine. Biochem Biophys Res Commun. 2000; 279(1): 69-73.

18. Barciszewski J, Siboska GE, Pedersen BO, Clark BF, Rattan SI: Evidence for the presence of kinetin in DNA and cell extracts. FEBS Lett. 1996; 393(2-3): 197-200.

19. Wyszko E, Barciszewska MZ, Markiewicz M, Szymański M, Markiewicz WT, Clark BF, Barciszewski J: "Action-at-a distance" of a new DNA oxidative damage product 6-furfuryl-adenine (kinetin) on template properties of modified DNA. Biochim Biophys Acta 2003;1625(3): 239-45.

20. Ge L, Yong JW, Goh NK, Chia LS, Tan SN, Ong ES: Identification of kinetin and kinetin riboside in coconut (Cocos nucifera L.) water using a combined approach of liquid chromatography-tandem mass spectrometry, high performance liquid chromatography and capillary electrophoresis. J Chromatogr B Analyt Technol Biomed Life Sci 2005; 829(1-2): 26-34.

21. Ge L, Yong JW, Tan SN, Ong ES: Determination of cytokinins in coconut (Cocos nucifera L.) water using capillary zone electrophoresis-tandem mass spectrometry. Electrophoresis 2006; 27(11): 2171-81.

22. Holland MA: Occam's Razor Applied to Hormonology (Are Cytokinins Produced by Plants?. Plant Physiol 1997; 115(3): 865-8.

23. Barciszewski J, Siboska G, Clark BFC, Rattan SIS: Cytokinin formation by oxidative metabolism. J Plant Physiol 2000; 157: 587–8.

24. Barciszewski J, Siboska GE, Pedersen BO, Clark BF, Rattan SI: A mechanism for the in vivo formation of N6-furfuryladenine, kinetin, as a secondary oxidative damage product of DNA. FEBS Lett. 1997; 414(2): 457-60.

25. Barciszewski J, Siboska GE, Pedersen BO, Clark BF, Rattan SI: Furfural, a precursor of the cytokinin hormone kinetin, and base propenals are formed by hydroxyl radical damage of DNA. Biochem Biophys Res Commun 1997; 238(2):317-9.

26. Björk GR, Ericson JU, Gustafsson CE, Hagervall TG, Jönsson YH, Wikström PM: Transfer RNA modification. Annu Rev Biochem 1987; 56: 263-87.

27. Chu HM, Ko TP, Wang AH: Crystal structure and substrate specificity of plant adenylate isopentenyltransferase from Humulus lupulus: distinctive binding affinity for purine and pyrimidine nucleotides. Nucleic Acids Res 2010; 38(5):1738-48.

28. Persson BC, Esberg B, Olafsson O, Björk GR: Synthesis and function of isopentenyl adenosine derivatives in tRNA. Biochimie 1994; 76(12): 1152-1160.

29. Buck M, Griffiths E: Regulation of aromatic amino acid transport by tRNA: role of 2-methylthio-N6-(delta2-isopentenyl)-adenosine. Nucleic Acids Res 1981; 9(2): 401-14.

30. Buck M, Ames BN: A modified nucleotide in tRNA as a possible regulator of aerobiosis: synthesis of cis-2-methyl-thioribosylzeatin in the tRNA of Salmonella. Cell 1984; 36(2): 523-31.

31. Urbonavicius J, Qian Q, Durand JM, Hagervall TG, Björk GR: Improvement of reading frame maintenance is a common function for several tRNA modifications. EMBO J 2001; 20(17): 4863-73.

32. Smith DW, Hatfield DL: Effects of post-transcriptional base modifications on the site-specific function of transfer RNA in eukaryote translation. J Mol Biol 1986; 189(4): 663-71.

33. Faust JR, Dice JF: Evidence for isopentenyladenine modification on a cell cycle-regulated protein. J Biol Chem 1991; 266(15): 9961-70.

34. Laten HM, Zahareas-Doktor S: Presence and source of free isopentenyladenosine in yeasts. Proc Natl Acad Sci USA 1985; 82(4): 1113-15.

35. Chen, C. M. (1982) in Plant Growth Substances 1982, ed. Wareing, P. F. (Academic, London), pp. 155-163.

36. Tanimoto S, Harada H: Effect of cytokinin and anticytokinin on the initial stage of adventitious bud differentiation in the epidermis of Torenia stem segments. Plant Cell Physiol 1982; 23: 1371–76.

37. Barry GF, Rogers SG, Fraley RT, Brand L: Identification of a cloned cytokinin biosynthetic gene. Proc Natl Acad Sci USA 1984; 81(15): 4776-80.

38. Mok M.C. (1994) in Cytokinins: Chemistry, Activity, and Function, eds Mok D. W. S., Mok M. C. (CRC Press, Boca Raton, FL), pp 155–166.

39. Ishii Y, Hori Y, Sakai S, Honma Y: Control of differentiation and apoptosis of human myeloid leukemia cells by cytokinins and cytokinin nucleosides, plant redifferentiation-inducing hormones. Cell Growth Differ 2002; 13(1): 19-26.

40. Gallagher R, Collins S, Trujillo J, McCredie K, Ahearn M, Tsai S, Metzgar R, Aulakh G, Ting R, Ruscetti F, Gallo R: Characterization of the continuous, differentiating myeloid cell line (HL-60) from a patient with acute promyelocytic leukemia. Blood 1979; 54(3): 713-33.

41. Sugimoto K, Yamada K, Egashira M, Yazaki Y, Hirai H, Kikuchi A, Oshimi K. Temporal and spatial distribution of DNA topoisomerase II alters during proliferation, differentiation, and apoptosis in HL-60 cells. Blood 1998; 91(4): 1407-17.

42. Mlejnek P, Dolezel P. Apoptosis induced by N6-substituted derivatives of adenosine is related to intracellular accumulation of corresponding mononucleotides in HL-60 cells. Toxicol In Vitro 2005; 19 (7): 985-90.

43. Gallo RC, Whang-Peng J, Perry S. Isopentenyladenosine stimulates and inhibits mitosis of human lymphocytes treated with phytohemagglutinin. Science 1969; 165(891): 400-2.

44. Divekar AY, Slocum HK, Hakala MT. N6-(delta2-isopentenyl)adenosine 5'-monophosphate: formation and effect on purine metabolism in cellular and enzymatic systems. Mol Pharmacol 1974; 10(3): 529-43.

45. Meisel H, Günther S, Martin D, Schlimme E. Apoptosis induced by modified ribonucleosides in human cell culture systems. FEBS Lett 1998; 433(3): 265-8.

46. Laezza C, Migliaro A, Cerbone R, Tedesco I, Santillo M, Garbi C, Bifulco M. N^6-isopentenyladenosine affects cAMP-dependent microfilament organization in FRTL-5 thyroid cells. Exp Cell Res 1997; 234(1): 178-82.

47. Laezza C, Notarnicola M, Caruso MG, Messa C, Macchia M, Bertini S, Minutolo F, Portella G, Fiorentino L, Stingo S, Bifulco M. N6-isopentenyladenosine arrests tumor cell proliferation by inhibiting farnesyl diphosphate synthase and protein prenylation. FASEB J 2006; 20(3): 412-8.

48. Spinola M, Galvan A, Pignatiello C, Conti B, Pastorino U, Nicander B, Paroni R, Dragani TA. Identification and functional characterization of the candidate tumor suppressor gene TRIT1 in human lung cancer. Oncogene 2005; 24(35): 5502-9.

49. Spinola M, Colombo F, Falvella FS, Dragani TA. N^6-isopentenyladenosine: a potential therapeutic agent for a variety of epithelial cancers. Int J Cancer 2007; 120(12): 2744-48.

50. Hoffman RM. In vitro sensitivity assays in cancer: a review, analysis, and prognosis. J Clin Lab Anal 1991; 5(2): 133-43.

51. Hamburger AW. The human tumor clonogenic assay as a model system in cell biology. Int J Cell Cloning 1987; 5(2): 89-107.

52. Laezza C, Caruso MG, Gentile T, Notarnicola M, Malfitano AM, Di Matola T, Messa C, Gazzerro P, Bifulco M. N^6-isopentenyladenosine inhibits cell proliferation and induces apoptosis in a human colon cancer cell line DLD1. Int J Cancer 2009; 124(6): 1322-29.

53. Griffaut B, Bos R, Maurizis JC, Madelmont JC, Ledoigt G. Cytotoxic effects of kinetin riboside on mouse, human and plant tumour cells. Int J Biol Macromol 2004; 34(4): 271-275.

54. Choi BH, Kim W, Wang QC, Kim DC, Tan SN, Yong JW, Kim KT, Yoon HS. Kinetin riboside preferentially induces apoptosis by modulating Bcl-2 family proteins and caspase-3 in cancer cells. Cancer Lett 2008; 261(1): 37-45.

55. Fidler IJ. Biological behavior of malignant melanoma cells correlated to their survival in vivo. Cancer Res 1975; 35(1): 218-224.

56. Engbring JA, Hoffman MP, Karmand AJ, Kleinman HK. The B16F10 cell receptor for a metastasis-promoting site on laminin-1 is a heparan

sulfate/chondroitin sulfate-containing proteoglycan. Cancer Res 2002; 62(12): 3549-54.

57. Shin DH, Kim OH, Jun HS, Kang MK. Inhibitory effect of capsaicin on B16-F10 melanoma cell migration via the phosphatidylinositol 3-kinase/Akt/Rac1 signal pathway. Exp Mol Med 2008; 40(5): 486-94.

58. Rahbari R, Sheahan T, Modes V, Collier P, Macfarlane C, Badge RM. A novel L1 retrotransposon marker for HeLa cell line identification. Biotechniques 2009; 46(4): 277-84.

59. Capes-Davis A, Theodosopoulos G, Atkin I, Drexler HG, Kohara A, MacLeod RA, Masters JR, Nakamura Y, Reid YA, Reddel RR, Freshney RI. Check your cultures! A list of cross-contaminated or misidentified cell lines. Int J Cancer 2010; 127(1): 1-8.

60. Tiedemann RE, Mao X, Shi CX, Zhu YX, Palmer SE, Sebag M, Marler R, Chesi M, Fonseca R, Bergsagel PL, Schimmer AD, Stewart AK. Identification of kinetin riboside as a repressor of CCND1 and CCND2 with preclinical antimyeloma activity. J Clin Invest 2008; 118(5): 1750-64.

61. Cabello CM, Bair WB 3rd, Ley S, Lamore SD, Azimian S, Wondrak GT. The experimental chemotherapeutic N^6-furfuryladenosine (kinetin-riboside) induces rapid ATP depletion, genotoxic stress, and CDKN1A(p21) upregulation in human cancer cell lines. Biochem Pharmacol 2009; 77(7): 1125-38.

62. Lynch HT, Albano WA, Heieck JJ, Mulcahy GM, Lynch JF, Layton MA, Danes BS. Genetics, biomarkers, and control of breast cancer: a review. Cancer Genet Cytogenet 1984; 13(1): 43-92.

63. Wolman SR, Smith HS, Stampfer M, Hackett AJ. Growth of diploid cells from breast cancers. Cancer Genet Cytogenet 1985;16(1): 49-64.

64. Orth JD, Tang Y, Shi J, Loy CT, Amendt C, Wilm C, Zenke FT, Mitchison TJ. Quantitative live imaging of cancer and normal cells treated with Kinesin-5 inhibitors indicates significant differences in phenotypic responses and cell fate. Mol Cancer Ther 2008; 7(11): 3480-89.

65. Tzioras S, Pavlidis N, Paraskevaidis E, Ioannidis JP. Effects of different chemotherapy regimens on survival for advanced cervical cancer: systematic review and meta-analysis. Cancer Treat Rev 2007; 33(1): 24-38.

66. Willmott N. Chemoembolization in regional cancer chemotherapy: a rationale. Cancer Treat Rev 1987; 14(2): 143-56.

67. Levenson AS, Jordan CV: MCF-7: the first hormone-responsive breast cancer cell line, Cancer Res 1997; 57(15): 3071-78.

68. Soule HD, Vazquez J, Long A, Albert S, Brennan M: A human cell line from a pleural effusion derived from a breast carcinoma, J Natl Cancer Inst 1973; 51(5): 1409-16.

69. Gooch JL, Yee D: Strain-specific differences in formation of apoptotic DNA ladder in MCF-7 breast cancer cells. Cancer Lett 1999; 144(1): 31-37.

70. Simstein R, Burow M, Parker A, Weldon C, Beckman B: Apoptosis, chemoresistance and breast cance: insights from the MCF-7 cell model system. Exp Biol Med 2003; 228(9): 995-1003.
71. Lacroix M, Leclercq G: Relevance of breast cancer cell lines as models for breast tumours: an update. Breast Cancer Res Treat 2004; 83(3): 249-89.
72. Jemal A, Murray T, Ward E, Samuels A, Tiwari RC, Ghafoor A, Feuer EJ, Thun MJ: Cancer statistics, 2005. CA Cancer J Clin 2005; 55: 10-30.
73. Pugacheva EN, Ivanov AV, Kravchenko JE, Kopnin BP, Levine AJ, Chumakov PM. Novel gain of function activity of p53 mutants: activation of the dUTPase gene expression leading to resistance to 5-fluorouracil. Oncogene 2002; 21: 4595-4600.
74. Swamy MV, Herzog CR, Rao CV. Inhibition of COX-2 in colon cancer cell lines by celecoxib increases the nuclear localization of active p53. Cancer Res 2003; 63: 5239-5242.
75. Bathaie SZ, Bolhasani A, Hoshyar R, Ranjbar B, Sabouni F, Moosavi-Movahedi AA: Interaction of saffron carotenoids as anticancer compounds with ctDNA, Oligo (dG.dC)15, and Oligo (dA.dT)15. DNA Cell Biol 2007; 26(8): 533-40.
76. Falkenberg M, Larsson NG, Gustafsson CM: DNA replication and transcription in mammalian mitochondria. Annu Rev Biochem 2007; 76: 679-99.
77. Levine AJ: p53, the cellular gatekeeper for growth and division. Cell 1997; 88(3): 323-31.
78. Imanishi Y: Molecular pathogenesis of tumorigenesis in sporadic parathyroid adenomas. J Bone Miner Metab 2002; 20(4):190-5.
79. Latchman DS: Transcription factors: an overview. Int J Biochem Cell Biol 1997; 29(12): 1305–12.
80. Karin M: Too many transcription factors: positive and negative interactions.New Biol 1990; 2(2): 126-31.
81. Roeder RG: The role of general initiation factors in transcription by RNA polymerase II. Trends Biochem Sci 1996; 21(9):327-35.
82. Nikolov DB, Burley SK: RNA polymerase II transcription initiation: a structural view. Proc Natl Acad Sci USA 1997; 94(1): 15-22.
83. Lee TI, Young RA: Transcription of eukaryotic protein-coding genes. Annu Rev Genet 2000; 34: 77–137.
84. Strekowski L, Wilson B: Noncovalent interactions with DNA: an overview.Mutat Res 2007; 623(1-2): 3-13.
85. Manning GS: The molecular theory of polyelectrolyte solutions with applications to the electrostatic properties of polynucleotides. Q Rev Biophys 1978;11(2):179-246.
86. Kanakis CD, Tarantilis PA, Pappas C, Bariyanga J, Tajmir-Riahi HA, Polissiou MG: An overview of structural features of DNA and RNA

complexes with saffron compounds: Models and antioxidant activity. J Photochem Photobiol B 2009; 95(3): 204-12.

87. Marsch GA, Ward RL, Colvin M, Turteltaub KW: Non-covalent DNA groove-binding by 2-amino-1-methyl-6-phenylimidazo[4,5-b]pyridine. Nucleic Acids Res 11; 22(24): 5408-15.

88. Dziegielewski J, Slusarski B, Konitz A, Skladanowski A, Konopa J: Intercalation of imidazoacridinones to DNA and its relevance to cytotoxic and antitumor activity. Biochem Pharmacol 2002; 63(9): 1653-62.

89. Traganos F, Kapuscinski J, Darzynkiewicz Z: Caffeine modulates the effects of DNA-intercalating drugs in vitro: a flow cytometric and spectrophotometric analysis of caffeine interaction with novantrone, doxorubicin, ellipticine, and the doxorubicin analogue AD198. Cancer Res 1991; 51(14): 3682-9.

90. Faddeeva MD, Beliaeva TN: DNA intercalators: their interaction with DNA and other cell components and their use in biological research. Tsitologiia 1991; 33(10): 3-31.

91. Ferguson LR, Denny WA: Genotoxicity of non-covalent interactions: DNA intercalators. Mutat Res 2007; 623(2): 14-23.

92. Snyder RD, Ewing D, Hendry LB. DNA intercalative potential of marketed drugs testing positive in in vitro cytogenetics assays. Mutat Res 2006; 609(1): 47-59. Epub 2006 Jul 20.

93. Beauchemin R, N'soukpoé-Kossi CN, Thomas TJ, Thomas T, Carpentier R, Tajmir-Riahi HA: Polyamine analogues bind human serum albumin. Biomacromolecules 2007; 8(10): 3177-83.

94. Kanakis CD, Tarantilis PA, Tajmir-Riahi HA, Polissiou MG: Crocetin, dimethylcrocetin, and safranal bind human serum albumin: stability and antioxidative properties. J Agric Food Chem 2007; 55(3): 970-977.

95. Froehlich E, Mandeville JS, Jennings CJ, Sedaghat-Herati R, Tajmir-Riahi HA: Dendrimers bind human serum albumin. J Phys Chem B 2009; 113(19): 6986-93.

96. Charbonneau D, Beauregard M, Tajmir-Riahi HA: Structural analysis of human serum albumin complexes with cationic lipids. J Phys Chem B. 12; 113(6): 1777-84.

97. Ercelen S, Klymchenko AS, Mély Y, Demchenko AP: The binding of novel two-color fluorescence probe FA to serum albumins of different species. Int J Biol Macromol 2005; 35(5): 231-42.

98. Hoang ND, Brecht K: Reactivity of isolated bovine facial vessels to electric stimulation and to drugs. Pharmacology 1979; 19(1): 23-35.

99. Kragh-Hansen U: Molecular aspects of ligand binding to serum albumin. Pharmacol Rev 1981; 33(1): 17-53.

100. Flarakos J, Morand KL, Vouros P: High-throughput solution-based medicinal library screening against human serum albumin. Anal Chem 2005; 77(5): 1345-53.

101. Bourassa P, Kanakis CD, Tarantilis P, Pollissiou MG, Tajmir-Riahi HA: Resveratrol, genistein, and curcumin bind bovine serum albumin. J Phys Chem B 2010;114(9): 3348-54.

102. Dubeau S, Bourassa P, Thomas TJ, Tajmir-Riahi HA: Biogenic and synthetic polyamines bind bovine serum albumin. Biomacromolecules 2010; 11(6): 1507-15.

103. Mandeville JS, Tajmir-Riahi HA: Complexes of dendrimers with bovine serum albumin. Biomacromolecules 2010; 11(2): 465-72.

104. Charbonneau DM, Tajmir-Riahi HA: Study on the interaction of cationic lipids with bovine serum albumin. J Phys Chem B. 2010; 114(2): 1148-55.

105. Chi Z, Liu R, Teng Y, Fang X, Gao C: Binding of oxytetracycline to bovine serum albumin: spectroscopic and molecular modeling investigations. J Agric Food Chem 2010; 58(18): 10262-69.

106. Paul BK, Samanta A, Guchhait N: Exploring hydrophobic subdomain IIA of the protein bovine serum albumin in the native, intermediate, unfolded, and refolded states by a small fluorescence molecular reporter. J Phys Chem B 2010; 114(18): 6183-96.

107. Banerjee T, Singh SK, Kishore N: Binding of naproxen and amitriptyline to bovine serum albumin: biophysical aspects. J Phys Chem B 2006; 110(47): 24147-56.

108. Georgiou ME, Georgiou CA, Koupparis MA: Automated flow injection gradient technique for binding studies of micromolecules to proteins using potentiometric sensors: application to bovine serum albumin with anilinonaphthalenesulfonate probe and drugs. Anal Chem 1999; 71(13): 2541-50.

109. Wu T, Wu Q, Guan S, Su H, Cai Z: Binding of the environmental pollutant naphthol to bovine serum albumin. Biomacromolecules 2007; 8(6): 1899-906.

110. Wang JYJ: DNA damage and apoptosis. Cell Death Diff 2001; 8: 1047-48.

111. Bagchi S, Raychaudhri P: Damaged-DNA Binding Protein-2 Drives Apoptosis Following DNA Damage. Cell Div 2010; 19(5): 3-5.

112. Mummery CL, van den Brink S, van der Saag PT, de Laat SW: Screening for cytotoxicity in neuroblastoma cells. I. Dependence of growth inhibition on the presence of serum. Toxicol Lett 1983; 18(3): 201-9.

113. Finlay GJ, Baguley BC: Effects of protein binding on the in vitro activity of antitumour acridine derivatives and related anticancer drugs. Cancer Chemother Pharmacol 2000; 45(5): 417-22.

114. Fischer AB: Factors influencing cadmium uptake and cytotoxicity in cultured cells. Xenobiotica 1985; 15(8-9): 751-757.

115. Robins MJ, Hall RH, Thedford R. N^6-(Δ^2-Isopentenyl)adenosine, a component of the transfer ribonucleic acid of yeast and of mammalian

tissue, methods of isolation, and characterization. Biochemistry 1967; 18486: 1837-1848.

116. Skehan P, Storeng R, Scudiero D, Monks A, McMahon J, Vistica D, Warren JT, Bokesch H, Kenney S, Boyd MR: New colorimetric cytotoxicity assay for anticancer-drug screening. J Natl Cancer Inst 1990; 82(13):1107-12.

117. Vichai V, Kirtikara K: Sulforhodamine B colorimetric assay for cytotoxicity screening. Nat Protoc 2006; 1(3): 1112-6.

118. Clarke PG, Clarke S: Nineteenth century research on naturally occurring cell death and related phenomena. Anat Embryol (Berl) 1996; 193(2): 81-99.

119. Ziegler U, Groscurth P: Morphological features of cell death. News Physiol Sci 2004; 19: 124-8.

120. Reed JC: Apoptosis-regulating proteins as targets for drug discovery. Tre Mol Med 2001; 7: 314–319.

121. Frankfurt OS, Krishan A: Apoptosis-based drug screening and detection of selective toxicity to cancer cells. Antican Drug 2003; 14: 555–561.

122. Pyle AM, Rehmann JP, Meshoyrer R, Kumar CV, Turro NJ, Barton JK: Mixed-ligand complexes of ruthenium(II): factors governing binding to DNA. J Am Chem Soc 1989; 111: 3053- 3058.

123. Tarushi A, Psomas G, Raptopoulou CP, Psycharis V, Kessissoglou DP: Structure and DNA-binding properties of bis(quinolonato)bis(pyridine)zinc(II) complexes. Polyhedron 2009; 28: 3272-3278.

124. Song YM, Wu Q, Yang PJ, Luan NN, Wang LF, Liu YM: DNA Binding and cleavage activity of Ni(II) complex with all-trans retinoic acid. J Inorg Biochem 2006; 100(10): 1685-91.

125. Long EC, Barton JK: On demonstrating DNA intercalation. Acc Chem Res 1990; 23(9): 271–273.

126. Psomas G. Mononuclear metal complexes with ciprofloxacin: Synthesis, characterization and DNA-binding properties. J Inorg Biochem 2008; 102(9):1798-811.

127. N'soukpoé-Kossi CN, Ouameur AA, Thomas T, Shirahata A, Thomas TJ, Tajmir-Riahi HA: DNA interaction with antitumor polyamine analogues: a comparison with biogenic polyamines. Biomacromolecules 2008; (10): 2712-8.

128. Makarska M, Pratviel G: Long-range charge transport through double-stranded DNA mediated by manganese or iron porphyrins. J Biol Inorg Chem 2008; 13(6): 973-979.

129. Uma V, Kanthimathi M, Weyhermuller T, Nair BU: Oxidative DNA cleavage mediated by a new copper (II) terpyridine complex: crystal structure and DNA binding studies. J Inorg Biochem 2005; 99(12): 2299-307.

130. Rajabi M, Gorincioi E, Santaniello E: N^6-Isopentenyladenosine, an isoprenoid cytokinin endowed with biological activity: cytotoxicity against MDA-MB-231 breast cancer cell line and interaction with bovine serum albumin. Iran J Org Chem 2010; 2(1): 278-284.

131. Kragh-Hansen U: Molecular aspects of ligand binding to serum albumin. Pharmacol Rev1981; 33(1): 17-53.

132. Klotz IM, Hunston DL: Properties of graphical representations of multiple classes of binding sites. Biochemistry 1971; 10(16): 3065-69.

133. Stephanos JJ: Drug-protein interactions: two-site binding of heterocyclic ligands to a monomeric hemoglobin. J Inorg Biochem 1996; 62(3): 155-69.

134. Zhong W, Wang Y, Yu JS, Liang Y, Ni K, Tu S: The interaction of human serum albumin with a novel antidiabetic agent-SU-118. J Pharm Sci 2004; 93(4): 1039-46.

135. Polyanichko AM, Andrushchenko VV, Chikhirzhina EV, Vorob'ev VI, Wieser H: The effect of manganese(II) on DNA structure: electronic and vibrational circular dichroism studies. Nucleic Acids Res 2004; 32(3): 989-96.

136. Andrushchenko V, Leonenko Z, Cramb D, van de Sande H, Wieser H: Vibrational CD (VCD) and atomic force microscopy (AFM) study of DNA interaction with Cr3+ ions: VCD and AFM evidence of DNA condensation. Biopolymers 2002; 61(4): 243-60.

137. Nafisi S, Manouchehri F, Tajmir-Riahi HA, Varavipour M: Structural features of DNA interaction with caffeine and theophylline. J Mol Strut 2008: 875; 392-399.

.